

**AN INVESTIGATION OF FLOW FIELD PERTURBATION CAUSED BY
CONSTANT BLADE TIP CLEARANCE IN A TURBINE**

by

Robert P. Gauthier

**B.S. Aeronautical and Astronautical Eng., MIT
1987**

**SUBMITTED TO THE DEPARTMENT OF
AERONAUTICAL AND ASTRONAUTICAL
ENGINEERING IN PARTIAL FULLFILLMENT OF THE
REQUIREMENTS FOR THE DEGREE OF**

MASTER OF SCIENCE

at the

MASSACHUSETTS INSTITUTE OF TECHNOLOGY

June 1990

**© Massachusetts Institute of Technology, 1990
All rights reserved**

Signature of Author

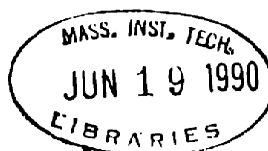
**Department of Aeronautical and Astronautical Engineering
March 1990**

Certified by

**Dr. Belgacem Jery
Assistant Professor, Aeronautical and Astronautical Engineering
Thesis Supervisor**

Accepted by

**Professor Harold Y. Wachman
Chairman, Graduate Thesis Committee**



ARCHIVES

**AN INVESTIGATION OF FLOW FIELD PERTURBATION CAUSED
BY CONSTANT BLADE TIP CLEARANCE IN A TURBINE**

by

Robert P. Gauthier

**Submitted to the Department of Aeronautics and Astronautics
on March, 1990 in partial fulfillment of the requirement
for the degree of Master of Science in
Aeronautics and Astronautics**

ABSTRACT

A turbine stage with constant blade-tip clearance is modelled by a two-dimensional actuator disk to investigate the flow field perturbation. It is solved analytically and numerically. The analytical solution uses inverse coordinates and a two-level velocity model. The numerical solution partitions the channel into a grid in the inverse coordinates and uses a pseudo-time marching technique on the non-linear model. For the two-level velocity model a shear layer forms at the blade tip and produces all the vorticity associated with the stage. This leads to constant axial velocities in both the blade and gap regions at the disc. The flow is therefore uniformly affected by the gap. Since these models overestimate the loss caused by the gap, two modifications were made to the two-level velocity model. First, variable density was introduced and was found to have only a small effect. Second, the theory of retained lift was used and significantly improved the results.

Thesis Supervisor: Dr. Belgacem Jery

Title: Assistant Professor of Aeronautical and Astronautical Engineering

ACKNOWLEDGMENTS

The author would like to thank Professor Manuel Martínez-Sánchez for his guidance and unending patience in the completion of this thesis. Thanks also to my friends Michael Gallagher and Steven Kowal for their continuous support and understanding. And finally special thanks to my parents for their love and encouragement.

TABLE OF CONTENTS

| | page |
|--|-------------|
| ABSTRACT | 2 |
| ACKNOWLEDGMENTS | 3 |
| TABLE OF CONTENTS | 4 |
| LIST OF SYMBOLS | 5 |
| | |
| 1. INTRODUCTION | 7 |
| 2. ANALYSIS | 9 |
| 2.2 Actuator Disk Model | 9 |
| 2.2.1(a) Transformation to Inverse Coordinates | 16 |
| 2.2.1(b) Two-Level Velocity Model | 18 |
| 2.2.2 Non-Linear Solution | 38 |
| 2.3 Modifications | 47 |
| 2.3.1 Compressible Flow | 48 |
| 2.3.2 Retained Lift | 55 |
| 3. RESULTS | 58 |
| 4. RECOMMENDATIONS | 61 |
| | |
| REFERENCES | 62 |
| FIGURES | 63 |
| TABLE | 90 |
| APPENDIX: COMPUTER PROGRAM | 91 |

LIST OF SYMBOLS

| | |
|------------------------------|--|
| B | Bernoulli constant |
| C | velocity |
| C_{x_0} | axial velocity far upstream |
| h | static enthalpy |
| H | total enthalpy or blade span |
| I | error from variation of equation |
| K | retained lift constant |
| P | pressure or power |
| Q | shear constant |
| R | reaction |
| U | blade speed |
| α | diffusivity |
| α_n | infinite series constants |
| α_2 | stator leaving angle |
| β_3 | relative rotor leaving angle |
| δ | gap size, variation of, or the delta function |
| λ | flow lost to gap |
| ω | vorticity |
| ψ | stream function |
| Ψ | work coefficient |
| ϕ | normalized stream function |
| Φ | flow coefficient |
| ρ | density |

Subscript

- 1 **stator inlet**
- 2 **stator exit and rotor inlet**
- 3 **rotor exit**
- ⊥ **In the x-z plane**
- T **at the blade tip**

Superscript

- ~ **perturbation**
- + **slightly above the blade tip**
- **slightly below the blade tip**

CHAPTER 1

INTRODUCTION

Vibrational instability is a major problem in high power turbomachinery. An example of this problem occurred in the Space Shuttle Main Engine turbopump system¹ during its initial testing. Vibrational instability creates shaft stresses that reduce fatigue life and can even cause catastrophic failure. The two major kinds of vibrational instabilities are forced and subsynchronous vibration. The first is due to rotor imbalance and is easily detected. Its vibrational frequencies are proportional to the shaft rotation speed. Subsynchronous vibration² can be the result of several things; hysteretic whirl³, dry friction whip⁴, fluid bearing whip and whirl⁵, seal forces⁶, and Alford force⁷ are some possibilities.

The most relevant to this thesis is the Alford force. This mechanism was discovered independently by Alford⁷ and Thomas⁸. It is considered one of the most important destabilizing forces because it is proportional to the turbomachine loading, which is being increased in more advanced turbomachine designs.

The Alford force is caused by variations of the blade-tip clearance. Turbine rotors should be perfectly centered with respect to the casing, and the blade-tip clearance held constant. In reality, however, the rotor will be slightly off-center. This creates a blade-tip clearance variation. Fluid passing through this varying tip clearance does no work, or at least reduced work and lowers the blade efficiency. Integrating the blade forces around the turbine produce a resultant force that is perpendicular to the shaft eccentricity. This destabilizing force is in the direction of the rotor rotation and thus produces a forward whirl.

Both the Alford and Thomas models ignore the effect of the flow disturbances created by the blade-tip variation. Steady flow is assumed, and the only effect of the blade-tip clearance variation is on the mass loss through the tip gap. This is an oversimplification that needs to be explored. Because the rotor blades are seen as a resistance to the flow, while the gap is not, the flow field will alter itself to allow more fluid to pass through the larger gap section. To simulate

this flow field disturbance a three-dimensional actuator disc model should be constructed. However, that is beyond the scope of this thesis, and instead a two-dimensional actuator disc model with constant tip leakage is used to investigate the flow perturbations due to the gap in the meridional plane. This is a continuation of the research of Yuan Qiu⁹ who investigated the effect of flow field perturbations of the Alford force by creating a two-dimensional actuator disc that distributed the effect of the gap over the blade, and solved for the flow disturbances in planes normal to the blades.

CHAPTER 2

ANALYSIS

2.1 Assumptions

In this analysis a turbine stage is represented by an actuator disk with constant blade-tip clearance. It is assumed that any perturbation of the flow is caused by this tip clearance. In developing this model the following assumptions were made:

- 1) Incompressible flow (for initial derivation)
- 2) constant axial velocity and two-dimensional geometry
- 3) no radial forces

The first assumption simplifies the analysis by assuming constant density. This implies the flow is restricted to low Mach numbers, and the pressure drops across the rotor are not large. Large pressure drops could result in choked flow and prevent downstream information from reaching upstream making this model useless. Incompressible flow is a fairly good assumption for some turbines since the Mach numbers are generally restricted to below .3. This assumption is removed in section 2.3.1.

Under steady conditions and constant density, constant axial velocity implies constant channel area by conservation of mass. But even under more general conditions, constant axial velocity is, by design, a common condition in real turbines. Even though real turbines have a significant change in channel area this simplification is made because it would be too difficult to solve otherwise. Also the error introduced by doing so is relatively small, and useful data can still be produced. Also by imposing two-dimensional geometry we can use simple rectangular coordinates. This is only valid for turbines with hub/tip ratios close to one.

2.2 Actuator Disk Model

Since the flow field is considered two-dimensional, the annular channel is unwrapped and

represented by a rectangular channel of height H (Fig. 2.1). The stator and rotor are shown as planes perpendicular to the flow, and the subscripts 1, 2, and 3 are used to denote upstream, between the stator and rotor, and downstream. The rotor gap, δ , is considered constant for this analysis.

The velocity triangles are shown in Fig. 2.2 where C is the absolute flow velocity and W is the relative flow velocity. The resulting y-velocities are

$$C_{y2} = C_x \tan \alpha_2 \quad (2.1a)$$

$$C_{y3} = U - C_x \tan \beta_3 \quad (2.1b)$$

where C_x is the axial velocity, U is the rotor velocity, and α_2 and β_3 are the flow angles.

The stream function, ψ , is introduced to satisfy continuity by

$$C_x = \frac{\partial \psi}{\partial z} \quad (2.2a)$$

$$C_z = -\frac{\partial \psi}{\partial x} \quad (2.2b)$$

Substituting the stream function into the vorticity equation gives

$$\nabla^2 \psi = \omega_y \quad (2.3)$$

Using conservation of momentum it can be shown that the C_y is convected downstream. Similarly ω_y is convected downstream and is therefore only a function of the stream function.

Because it is assumed there is uniform irrotational flow upstream of the blades, the vorticity is zero. Thus the governing equation there is the Laplace equation

$$\nabla^2 \psi = 0 \quad (2.4)$$

Downstream, however, the flow is rotational. The blades and rotor gap produce vorticity which is carried downstream. The governing equation downstream of the blades is therefore the non-linear Poisson equation

$$\nabla^2 \psi = \omega_y(\psi) \quad (2.5)$$

The function $\omega_y(\psi)$ is determined by the boundary conditions imposed by the stage. To find a useful form of the vorticity we first take the two-dimensional part of the momentum equation.

$$\nabla \left(\frac{C_{\perp}^2}{2} + \frac{P}{\rho} \right) + \vec{\omega} \times \vec{C}_{\perp} = 0 \quad (2.6)$$

where

$$C_{\perp}^2 = C_x^2 + C_y^2 \quad (2.7)$$

Next take the dot product of the equation with the normal vector and make the substitution

$$\frac{\partial}{\partial n} = C_{\perp} \frac{\partial}{\partial \psi} \quad (2.8)$$

which gives

$$\omega_y = \frac{\partial}{\partial \psi} \left(\frac{C_{\perp}^2}{2} + \frac{P}{\rho} \right) \quad (2.9)$$

The quantity in the parenthesis is the Bernoulli constant, B_{\perp} , which is constant along streamlines, and is set by the stage parameters. Since the flow is uniform upstream

$$\frac{\partial B_{\perp}}{\partial \psi} = 0 \quad (2.10)$$

Downstream $B_{\perp 3}$ is given by

$$B_{\perp 3} = \frac{1}{2} (C_{x_3}^2 + C_{z_3}^2) + \frac{P_3}{\rho} \quad (2.11)$$

Since the velocities before and after the disk approach the same values at the disk, equation (2.11) can be written

$$B_{\perp 3} = \frac{1}{2} (C_{x_1}^2 + C_{z_1}^2) + \frac{P_3}{\rho} \quad (2.12)$$

By adding and subtracting P_1/ρ

$$B_{\perp 3} = \frac{1}{2} (C_{x_1}^2 + C_{z_1}^2) + \frac{P_1}{\rho} - \frac{P_1 - P_3}{\rho} \quad (2.13)$$

a substitution can be made with $B_{\perp 1}$

$$B_{\perp 3} = B_{\perp 1} - \frac{P_1 - P_3}{\rho} \quad (2.14)$$

Taking the derivative with respect to ψ and using equation (2.10) gives

$$\frac{\partial B_{13}}{\partial \psi} = - \frac{\partial}{\partial \psi} \left(\frac{P_1 - P_3}{\rho} \right) \quad (2.15)$$

Now the pressure drop is calculated across the blade row. For the portion of the flow that passes through both the stator and rotor we use the isentropic substitution

$$h_1 - h_3 = \frac{P_1 - P_3}{\rho} \quad (2.16)$$

and the Euler turbine equation to get

$$\frac{P_1 - P_3}{\rho} = UC_x \tan \alpha_2 - \frac{1}{2} (U^2 - C_x^2 \tan^2 \beta_3) \quad (2.17)$$

The rest of the flow must pass through the rotor gap. Since the gap itself is assumed to have no resistance to the flow, all the pressure drop must occur across the stator. No energy is extracted from this fluid so we can use Bernoulli's equation to calculate the pressure drop. Note that this is not strictly correct, since some of the gap streamtubes are partially deflected and do a fraction of the work done by the streamtubes far from the gap. This will be reconsidered in section 2.3.2. For now we set

$$\frac{P_1 - P_3}{\rho} = \frac{1}{2} \tan^2 \alpha_2 \quad (2.18)$$

Now we substitute equations (2.17) and (2.18) into equation (2.15) and make a change of variables using

$$\frac{\partial}{\partial \psi} = \frac{1}{C_x} \left(\frac{\partial C_x}{\partial z} \right)_{x=0} \left(\frac{\partial}{\partial C_x} \right) \quad (2.19)$$

Taking the derivative with respect to C_x gives the resulting equations.

$$\text{BLADE:} \quad \omega_y = - \left[\frac{U}{(C_x)_{x=0}} \tan \alpha_2 + \tan^2 \beta_3 \right] \left(\frac{\partial C_x}{\partial z} \right)_{x=0} \quad (2.20a)$$

$$\text{GAP:} \quad \omega_y = - \left[\tan^2 \alpha_2 \right] \left(\frac{\partial C_x}{\partial z} \right)_{x=0} \quad (2.20b)$$

The vorticity in the blade and gap regions can now be calculated, but the discontinuity at the blade tip produces a shear layer. To find the strength of the shear layer we integrate the vorticity across the the blade tip to get

$$\int \omega_y \partial \psi = B_{\perp,1}^+ - B_{\perp,1}^- \quad (2.21)$$

where $B_{\perp_3}^+$ and $B_{\perp_3}^-$ are the Bernoulli constants just above and just below the blade tip. By substituting in the values of these Bernoulli constants we get the result

$$\int \omega_y \partial\psi = U C_x^- \tan \alpha_2 - \frac{1}{2} \left(U^2 - C_x^{-2} \tan^2 \beta_3 \right) - \frac{1}{2} C_x^{+2} \tan^2 \alpha_2 \quad (2.22)$$

which means the vorticity produced by the shear layer is

$$\omega_y = \left[U C_x^- \tan \alpha_2 - \frac{1}{2} \left(U^2 - C_x^{-2} \tan^2 \beta_3 \right) - \frac{1}{2} C_x^{+2} \tan^2 \alpha_2 \right] \delta(\psi - \psi_T) \quad (2.23)$$

where ψ_T is the streamline that passes through the blade tip. Substituting equations (2.20a), (2.20b) and (2.23) into equation (2.5) gives the governing equation for the downstream region. The governing equations are solved in two ways. The first is an analytic approach which uses inverse coordinates and a two-level velocity model. The second is a non-linear numerical approach using inverse coordinates and a pseudo-time marching technique.

2.2.1(a) Transformation to Inverse Coordinates

Since the forcing term in the governing equation is a function of the stream function a change of coordinate is made from (x,z) to (x,ψ) . The axial and radial velocities are now represented by

$$C_x = \frac{1}{\left(\frac{\partial z}{\partial \psi}\right)} \quad (2.24a)$$

$$C_z = \frac{\left(\frac{\partial z}{\partial x}\right)}{\left(\frac{\partial z}{\partial \psi}\right)} \quad (2.24b)$$

and the Laplacian becomes

$$\nabla^2 \psi = \frac{1}{Z_\psi^3} \left[-Z_\psi^2 Z_{xx} + 2Z_x Z_\psi Z_{x\psi} - (1 + Z_x^2) Z_{\psi\psi} \right] \quad (2.25)$$

where the subscripts represent the partial derivatives of Z with respect to that subscript. With the additional substitution

$$\left(\frac{\partial C_x}{\partial z}\right)_{x=0} = - \left(\frac{Z_{\psi\psi}}{Z_\psi^3}\right)_{x=0} \quad (2.26)$$

the governing equations can be written

UPSTREAM:

$$-\frac{1}{Z_\psi^3} \left[Z_\psi^2 Z_{xx} - 2Z_x Z_\psi Z_{x\psi} + (1 + Z_x^2) Z_{\psi\psi} \right] = 0 \quad (2.27a)$$

DOWNSTREAM:

$$-\frac{1}{Z_\psi^3} \left[Z_\psi^2 Z_{xx} - 2Z_x Z_\psi Z_{x\psi} + (1 + Z_x^2) Z_{\psi\psi} \right] =$$

$$\left\{ \begin{array}{ll} \left[\tan^2 \alpha_2 \right] \left(\frac{Z_{\psi\psi}}{Z_\psi^3} \right)_{x=0} & \psi_T < \psi < HC_{x_0} \\ \left[U C_x^- \tan \alpha_2 - \frac{1}{2} (U^2 - C_x^{-2} \tan^2 \beta_3) - \frac{1}{2} C_x^{+2} \tan^2 \alpha_2 \right] \delta(\psi - \psi_T) & \\ \left[U (Z_\psi)_{x=0} \tan \alpha_2 + \tan^2 \beta_3 \right] \left(\frac{Z_{\psi\psi}}{Z_\psi^3} \right)_{x=0} & 0 < \psi < \psi_T \end{array} \right. \quad (2.27b)$$

2.2.1(b) Two-Level Velocity Model

These equations are highly non-linear and impossible to solve exactly by analytical means. They are, therefore, linearized using

$$Z = \frac{\psi}{C_{x_0}} + \tilde{Z} \quad (2.28)$$

where \tilde{Z} is the perturbation of Z . Now the axial and radial velocities become

$$C_x = C_{x_0} - C_{x_0}^2 \tilde{Z}_\psi \quad (2.29a)$$

$$C_x = C_{x_0} \tilde{Z}_x \quad (2.29b)$$

After calculating the partial derivatives of Z in terms of \tilde{Z} , neglecting terms higher than linear in \tilde{Z} , and dividing through by $-C_{x_0}^3$, the governing equations become

UPSTREAM:

$$\frac{1}{C_{x_0}^2} \tilde{Z}_{xx} + \tilde{Z}_{\psi\psi} = 0 \quad (2.30a)$$

DOWNSTREAM:

$$\frac{1}{C_{x_0}^2} \tilde{Z}_{xx} + \tilde{Z}_{\psi\psi} = \begin{cases} - [\tan^2 \alpha_2] (\tilde{Z}_{\psi\psi})_{x=0} & \psi_T < \psi < HC_{x_0} \\ -\frac{1}{2C_{x_0}} \left[\frac{2}{\Phi} \left(\frac{C_x^-}{C_{x_0}} \right) \tan \alpha_2 - \frac{1}{\Phi^2} + \left(\frac{C_x^-}{C_{x_0}} \right)^2 \tan^2 \beta_3 - \left(\frac{C_x^+}{C_{x_0}} \right)^2 \tan^2 \alpha_2 \right] \delta(\psi - \psi_T) & \\ - \left[\frac{1}{\Phi} \tan \alpha_2 + \tan^2 \beta_3 \right] (\tilde{Z}_{\psi\psi})_{x=0} & 0 < \psi < \psi_T \end{cases} \quad (2.30b)$$

where Φ is defined as the flow coefficient, i.e., $\Phi = C_{x_0}/U$. Note that the velocities in the shear

layer term are not fully linearized, but instead are piecewise constant. The ratios C_x^-/C_{x_0} and C_x^+/C_{x_0} will be solved for later.

To solve the Laplace-Poisson governing equation we need to impose the boundary conditions.

| | | |
|---------------|---|---|
| 1) Lower wall | $Z(\psi=0) = 0$ | $\tilde{Z}(\psi=0) = 0$ |
| 2) Upper wall | $Z(\psi=HC_{x_0}) = H$ | $\tilde{Z}(\psi=HC_{x_0}) = 0$ |
| 3) Upstream | $\psi(x \rightarrow -\infty) \rightarrow C_{x_0} Z$ | $\tilde{Z} \rightarrow 0$ as $x \rightarrow -\infty$ |
| 4) Downstream | $C_z = -\frac{\partial \Psi}{\partial x}(x \rightarrow \infty) \rightarrow 0$ | $\tilde{Z}_x \rightarrow 0$ as $x \rightarrow \infty$ |
| 5) At disk | C_x, C_z continuous | $\tilde{Z}_x, \tilde{Z}_\psi, \tilde{Z}$ continuous |

It can be shown that solutions of the following form satisfy all five boundary conditions (as well as the governing equation for $x < 0$).

$$\frac{\tilde{Z}}{H} = \sum_{n=1}^{\infty} \alpha_n e^{\frac{n\pi x}{H}} \sin n\pi\phi \quad x < 0 \quad (2.31a)$$

$$\frac{\tilde{Z}}{H} = \sum_{n=1}^{\infty} \alpha_n \left(2 - e^{-\frac{n\pi x}{H}} \right) \sin n\pi\phi \quad x > 0 \quad (2.31b)$$

where ϕ is the non-dimensional form of the stream function given by

$$\phi = \frac{\psi}{HC_{x_0}} \quad (2.32)$$

The following analysis shows how the constants α_n were determined. First, the Bernoulli constant was written in its velocity components and pressure form. Then its derivative with respect to ψ was taken at $x \rightarrow \infty$, and the C_x was replaced by its definition from conservation of mass.

$$\left(\frac{\partial B_{\perp 3}}{\partial \psi} \right)_{x=\infty} = \left(C_x \frac{\partial C_x}{\partial \psi} \right)_{x=\infty} = \left(\frac{\partial C_x}{\partial Z} \right)_{x=\infty} \quad (2.33)$$

At $x=0$ the derivative of the Bernoulli constant with respect to ψ has already been found and is given by

$$\left(\frac{\partial B_{\perp 3}}{\partial \psi} \right)_{x=0} = F(\psi) \left(\frac{\partial C_x}{\partial Z} \right)_{x=0} \quad (2.34)$$

where $F(\psi)$ is given by the equations (2.20a) and (2.20b). Since the Bernoulli constant is constant along streamlines, its derivative with respect to ψ at the disc should be equal to its derivative with respect to ψ at infinity.

$$\left(\frac{\partial B_{\perp 3}}{\partial \psi} \right)_{x=\infty} = \left(\frac{\partial B_{\perp 3}}{\partial \psi} \right)_{x=0} \quad (2.35)$$

This leads to

$$\left(\frac{\partial C_x}{\partial Z} \right)_{x=\infty} = F(\psi) \left(\frac{\partial C_x}{\partial Z} \right)_{x=0} \quad (2.36)$$

Linearized actuator disks have a common property of distributing the perturbation evenly so that the perturbation at infinity is twice the perturbation at the disk.¹¹ If we assume this, then it follows

$$\left(\frac{\partial C_x}{\partial Z}\right)_{x=\infty} = 2 \left(\frac{\partial C_x}{\partial Z}\right)_{x=0} \quad (2.37)$$

The only way to satisfy both of the previous equations is if 1) $F(\psi)=2$, which is generally impossible except for some exceptional conditions, or 2)

$$\left(\frac{\partial C_x}{\partial Z}\right)_{x=0} = 0 \quad (2.38)$$

This means that $(C_x)_{x=0}$ is a constant for both the blade and gap regions with a discontinuity at the blade tip (Fig 2.3).

The Fourier cosine expansion for something of this shape gives the form of the constants α_n . The velocity perturbations in the axial direction must sum to zero to satisfy continuity. This gives (with $\phi_T = \psi_T / (C_{x_0} H) = 1 - \lambda$)

$$\lambda \bar{Z}_\psi^+ + (1 - \lambda) \bar{Z}_\psi^- = 0 \quad (2.39)$$

Anywhere on the shear layer (in particular when $x \rightarrow \infty$) we have

$$\bar{Z}_\psi^+ - \bar{Z}_\psi^- = -\frac{Q}{2C_{x_0}} \quad \phi = \phi_T \quad (2.40)$$

where Q is defined from equation (2.30b) as

$$Q = \frac{2}{\Phi} \left(\frac{C_x^-}{C_{x_0}} \right) \tan \alpha_2 - \frac{1}{\Phi^2} + \left(\frac{C_x^-}{C_{x_0}} \right)^2 \tan^2 \beta_3 - \left(\frac{C_x^+}{C_{x_0}} \right)^2 \tan^2 \alpha_2 \quad (2.41)$$

If the quantity $\tilde{Z}_\psi^+ - \tilde{Z}_\psi^-$ is evaluated at the disk, a factor of 1/2 must be introduced to reflect the general property of linearized actuator disk theory that the perturbation on the disk is 1/2 that downstream.

$$\left(\tilde{Z}_\psi^+ - \tilde{Z}_\psi^- \right)_{x=0} = -\frac{Q}{4C_{x_0}} \quad \phi = \phi_T \quad (2.42)$$

Combining equations (2.39) and (2.42) gives

$$\bar{Z}_\psi^+ = -\frac{(1-\lambda)Q}{4C_{x_0}} \quad (2.43a)$$

$$\bar{Z}_\psi^- = \frac{\lambda Q}{4C_{x_0}} \quad (2.43b)$$

By taking the derivative of equation (2.31a) with respect to ψ and evaluating it at the disk we get

$$\left(\bar{Z}_\psi\right)_{x=0} = \frac{\pi}{C_{x_0}} \sum_{n=1}^{\infty} n \alpha_n \cos n\pi\phi \quad (2.44)$$

Using Fourier analysis with a cosine expansion of \tilde{Z}_ψ over the interval $(-1,1)$ gives

$$\int_{-1}^1 \bar{Z}_\psi \cos m\pi\phi d\phi = \frac{\pi}{C_{x_0}} \sum_{n=1}^{\infty} n \alpha_n \int_{-1}^1 \cos n\pi\phi \cos m\pi\phi d\phi = \frac{\pi}{C_{x_0}} m \alpha_m \quad (2.45a)$$

Taking the same integral but using equations (2.43a) and (2.43b) for \tilde{Z}_ψ gives

$$\begin{aligned} \int_{-1}^1 \bar{Z}_\psi \cos m\pi\phi d\phi &= 2 \left(\int_0^{\phi_T} \frac{\lambda Q}{4C_{x_0}} \cos m\pi\phi d\phi + \int_{\phi_T}^1 -\frac{(1-\lambda) Q}{4C_{x_0}} \cos m\pi\phi d\phi \right) \\ &= \frac{Q}{2C_{x_0}} \frac{\sin m\pi\phi_T}{m\pi} \end{aligned} \quad (2.45b)$$

Now equating the two previous equations gives us the solution for α_n

$$\alpha_n = \frac{Q}{2\pi^2} \frac{\sin n\pi\phi_T}{n^2} \quad (2.46)$$

where ϕ_T is ϕ evaluated at the blade tip. If we define the non-dimensional flow lost to the gap as

$$\lambda = 1 - \phi_T \quad (2.47)$$

then equation (2.46) can be rewritten

$$\alpha_n = (-1)^{n+1} \frac{Q}{2\pi^2} \frac{\sin n\pi\lambda}{n^2} \quad (2.48)$$

and the non-dimensional size of the gap can be found from equation (2.31a), using $x=0$, $\phi=1-\lambda$, and $\tilde{Z}_{tip}=H(\lambda-\delta)$ with the help of the infinite series solution

$$\sum_{n=1}^{\infty} \frac{\sin^2 n\pi\lambda}{n^2} = \frac{\pi^2}{2} \lambda (1 - \lambda) \quad (2.49)$$

which gives the result

$$\frac{\delta}{H} = \lambda \left[1 - \frac{Q}{4} (1 - \lambda) \right] \quad (2.50)$$

Since we can't solve for the perturbations exactly for the rest of the channel, we turn to the

derivatives of \tilde{Z} which we can solve exactly. For the upstream region the derivatives of \tilde{Z} with respect to x and ψ are

$$\tilde{Z}_x = \pi \sum_{n=1}^{\infty} n \alpha_n e^{\frac{n\pi x}{H}} \sin n\pi\phi \quad (2.51a)$$

$$\tilde{Z}_\psi = \frac{\pi}{C_{x_0}} \sum_{n=1}^{\infty} n \alpha_n e^{\frac{n\pi x}{H}} \cos n\pi\phi \quad (2.51b)$$

Plugging in equation (2.48) gives

$$\tilde{Z}_x = \frac{Q}{2\pi} \sum_{n=1}^{\infty} (-1)^{n+1} e^{\frac{n\pi x}{H}} \frac{\sin n\pi\lambda \sin n\pi\phi}{n} \quad (2.52a)$$

$$\tilde{Z}_\psi = \frac{Q}{2\pi C_{x_0}} \sum_{n=1}^{\infty} (-1)^{n+1} e^{\frac{n\pi x}{H}} \frac{\sin n\pi\lambda \cos n\pi\phi}{n} \quad (2.52b)$$

Now we use the trigonometric substitutions

$$(-1)^{n+1} \sin n\pi\phi = \sin n\pi(1-\phi) \quad (2.53a)$$

$$(-1)^n \cos n\pi\phi = \cos n\pi(1-\phi) \quad (2.53b)$$

to get

$$\tilde{Z}_x = \frac{Q}{2\pi} \sum_{n=1}^{\infty} e^{\frac{n\pi z}{H}} \frac{\sin n\pi\lambda \sin n\pi(1-\phi)}{n} \quad (2.54a)$$

$$\tilde{Z}_\psi = -\frac{Q}{2\pi C_{x_0}} \sum_{n=1}^{\infty} e^{\frac{n\pi z}{H}} \frac{\sin n\pi\lambda \cos n\pi(1-\phi)}{n} \quad (2.54b)$$

This can be manipulated again using trigonometric substitutions to get

$$\tilde{Z}_x = \frac{Q}{4\pi} \sum_{n=1}^{\infty} e^{\frac{n\pi z}{H}} \frac{\cos n\pi(1-\phi-\lambda) - \cos n\pi(1-\phi+\lambda)}{n} \quad (2.55a)$$

$$\tilde{Z}_\psi = \frac{Q}{4\pi C_{x_0}} \sum_{n=1}^{\infty} e^{\frac{n\pi z}{H}} \frac{\sin n\pi(1-\phi-\lambda) - \sin n\pi(1-\phi+\lambda)}{n} \quad (2.55b)$$

With the help of the following infinite series solutions

$$\sum_{n=1}^{\infty} \frac{p^n \cos ny}{n} = \ln \left[\frac{1}{\sqrt{1 - 2p \cos y + p^2}} \right] \quad (2.56a)$$

$$\sum_{n=1}^{\infty} \frac{p^n \sin ny}{n} = \tan^{-1} \left[\frac{p \sin y}{1 - p \cos y} \right] \quad (2.56b)$$

the derivatives of \tilde{Z} for $x < 0$ become

$$\tilde{Z}_x = \frac{Q}{8\pi} \ln \left[\frac{1 - 2e^{\frac{\pi\psi}{H}} \cos \pi(1-\phi+\lambda) + e^{\frac{2\pi\psi}{H}}}{1 - 2e^{\frac{\pi\psi}{H}} \cos \pi(1-\phi-\lambda) + e^{\frac{2\pi\psi}{H}}} \right] \quad (2.57a)$$

$$\tilde{Z}_\psi = \frac{Q}{4\pi C'_{x_0}} \left\{ \tan^{-1} \left[\frac{\sin \pi(1-\phi-\lambda)}{e^{-\frac{\pi\psi}{H}} - \cos \pi(1-\phi-\lambda)} \right] - \tan^{-1} \left[\frac{\sin \pi(1-\phi+\lambda)}{e^{-\frac{\pi\psi}{H}} - \cos \pi(1-\phi+\lambda)} \right] \right\} \quad (2.57b)$$

For the downstream solution we get

$$\tilde{Z}_x = \frac{Q}{8\pi} \ln \left[\frac{1 - 2e^{-\frac{\pi\psi}{H}} \cos \pi(1-\phi+\lambda) + e^{-\frac{2\pi\psi}{H}}}{1 - 2e^{-\frac{\pi\psi}{H}} \cos \pi(1-\phi-\lambda) + e^{-\frac{2\pi\psi}{H}}} \right] \quad (2.58)$$

It is the same as the upstream solution except the exponent has changed sign. The derivative of \tilde{Z} with respect to ψ for the downstream section is a little more difficult to find because it has two parts.

$$\tilde{Z}_\psi = \frac{\pi}{C_{x_0}} \sum_{n=1}^{\infty} n \alpha_n \left(2 - e^{-\frac{n\pi x}{H}} \right) \cos n\pi\phi \quad (2.59)$$

The first term can be rewritten by inserting equation (2.48)

$$\frac{2\pi}{C_{x_0}} \sum_{n=1}^{\infty} n \alpha_n \cos n\pi\phi = \frac{Q}{\pi C_{x_0}} \sum_{n=1}^{\infty} (-1)^{n+1} \frac{\sin n\pi\lambda \cos n\pi\phi}{n} \quad (2.60)$$

This is the same as the upstream solution (2.52b) except it is multiplied by two and doesn't have the exponential. So the first part of the downstream solution for the derivative of \tilde{Z} with respect to ψ is (from 2.57b)

$$\begin{aligned} & \frac{2\pi}{C_{x_0}} \sum_{n=1}^{\infty} n \alpha_n \cos n\pi\phi = \\ & \frac{Q}{2\pi C_{x_0}} \left\{ \tan^{-1} \left[\frac{\sin \pi (1-\phi-\lambda)}{1 - \cos \pi (1-\phi-\lambda)} \right] - \tan^{-1} \left[\frac{\sin \pi (1-\phi+\lambda)}{1 - \cos \pi (1-\phi+\lambda)} \right] \right\} \end{aligned} \quad (2.61)$$

Using the trigonometric substitutions

$$\frac{\sin \theta}{1 - \cos \theta} = \frac{1}{\tan \frac{\theta}{2}} \quad (2.62)$$

and

$$\tan^{-1} \left(\frac{1}{\tan \frac{\theta}{2}} \right) = \frac{\pi}{2} - \frac{\theta}{2} \quad (2.63)$$

we get the result

$$\frac{2\pi}{C_{x_0}} \sum_{n=1}^{\infty} n \alpha_n \cos n\pi\phi = \frac{Q}{2\pi C_{x_0}} \begin{cases} -\pi(1-\lambda) & \phi_r < \phi < 1 \\ \pi\lambda & 0 < \phi < \phi_r \end{cases} \quad (2.64)$$

The discontinuity is caused by the first term on the right hand side of equation (2.61) which jumps from $\pi/2$ to $-\pi/2$ at $\phi = 1-\lambda$. This is shown in Fig 2.4. The second part of the derivative of \tilde{Z} with respect to ψ is the same as the upstream solution except the exponent and the terms change sign. Combining the solutions for the two parts gives for $x>0$

$$\begin{aligned} \dot{\tilde{Z}}_{\psi} = \frac{Q}{4\pi C_{x_0}} \left\{ \left[\frac{-2\pi(1-\lambda)}{2\pi\lambda} \right] - \tan^{-1} \left[\frac{\sin \pi(1-\phi-\lambda)}{e^{\frac{\pi\psi}{H}} - \cos \pi(1-\phi-\lambda)} \right] + \right. \\ \left. \tan^{-1} \left[\frac{\sin \pi(1-\phi+\lambda)}{e^{\frac{\pi\psi}{H}} - \cos \pi(1-\phi+\lambda)} \right] \right\} \quad (2.65) \end{aligned}$$

At the disc the derivative of \tilde{Z} with respect to x and ψ become (from 2.57a and 2.57b)

$$(\tilde{Z}_x)_{x=0} = \frac{Q}{8\pi} \ln \left[\frac{2 - 2 \cos \pi (1 - \phi + \lambda)}{2 - 2 \cos \pi (1 - \phi - \lambda)} \right] \quad (2.66a)$$

$$(\tilde{Z}_\psi)_{x=0} = \frac{Q}{4\pi C_{x_0}} \left\{ \tan^{-1} \left[\frac{\sin \pi (1 - \phi - \lambda)}{1 - \cos \pi (1 - \phi - \lambda)} \right] - \tan^{-1} \left[\frac{\sin \pi (1 - \phi + \lambda)}{1 - \cos \pi (1 - \phi + \lambda)} \right] \right\} \quad (2.66b)$$

which simplify to

$$(\tilde{Z}_x)_{x=0} = \frac{Q}{4\pi} \ln \left[\frac{\sin \frac{\pi}{2} (1 - \phi + \lambda)}{\sin \frac{\pi}{2} (1 - \phi - \lambda)} \right] \quad (2.67a)$$

$$(\tilde{Z}_\psi)_{x=0} = \frac{Q}{4C_{x_0}} \begin{cases} -(1 - \lambda) & \phi_T < \phi < 1 \\ \lambda & 0 < \phi < \phi_T \end{cases} \quad (2.67b)$$

This last equation is indeed of the right form (see Eqs. 2.43a,b). Since we defined the radial and axial velocities in equations (2.29a) and (2.29b) we can calculate the velocities at the disk

$$C_z = \frac{QC_{x_0}}{4\pi} \ln \left[\frac{\sin \frac{\pi}{2} (1 - \phi + \lambda)}{\sin \frac{\pi}{2} (1 - \phi - \lambda)} \right] \quad (2.68a)$$

$$C_x = C_{x_0} \begin{cases} 1 + \frac{Q}{4}(1 - \lambda) & \phi_T < \phi < 1 \\ 1 - \frac{Q}{4}\lambda & 0 < \phi < \phi_T \end{cases} \quad (2.68b)$$

The axial velocity is not a function of ϕ and is constant in the blade and gap regions. This means

$$\left(\frac{\partial C_x}{\partial Z} \right)_{x=0} = 0 \quad \phi \neq \phi_T \quad (2.69)$$

and the vorticity is only produced by a shear layer at the blade tip. Thus the governing equations simplify to

$$\text{UPSTREAM:} \quad \frac{1}{C_{x_0}^2} \tilde{Z}_{xx} + \tilde{Z}_{\psi\psi} = 0 \quad (2.70a)$$

$$\text{DOWNSTREAM:} \quad \frac{1}{C_{x_0}^2} \tilde{Z}_{xx} + \tilde{Z}_{\psi\psi} = -\frac{Q}{2C_{x_0}} \delta(\psi - \psi_T) \quad (2.70b)$$

We can now solve for Q by using equation (2.68b) to find the velocity ratios, C_x^+/C_{x_0} and C_x^-/C_{x_0} in terms of Q and substituting these into equation (2.41). This gives the quadratic equation

$$\begin{aligned}
 & Q^2 \left[\frac{\lambda^2}{16} \tan^2 \beta_3 - \frac{(1-\lambda)^2}{16} \tan^2 \alpha_2 \right] + \\
 & Q \left[-\frac{(1-\lambda)}{2} \tan^2 \alpha_2 - \frac{\lambda}{2\Phi} \tan \alpha_2 - \frac{\lambda}{2} \tan^2 \beta_3 - 1 \right] + \\
 & \left[\frac{2}{\Phi} \tan \alpha_2 - \frac{1}{\Phi^2} + \tan^2 \beta_3 - \tan^2 \alpha_2 \right] = 0
 \end{aligned} \tag{2.71}$$

that can be solved for Q.

To solve for the streamline that passes through the blade tip we start with (see equation (2.58) with $\phi=1-\lambda$)

$$\bar{Z}_x(\phi_T, x > 0) = \frac{Q}{8\pi} \ln \left[\frac{1 - 2e^{-\frac{\pi x}{H}} \cos 2\pi\lambda + e^{-\frac{2\pi x}{H}}}{(1 - e^{-\frac{\pi x}{H}})^2} \right] \tag{2.72}$$

which can be rewritten

$$\bar{Z}_x(\phi_T, x > 0) = \frac{Q}{8\pi} \ln \left[1 + \frac{2(1 - \cos 2\pi\lambda) e^{-\frac{\pi x}{H}}}{(1 - e^{-\frac{\pi x}{H}})^2} \right] \tag{2.73}$$

This is not integrable analytically, but for λ small and $x \gg H\lambda$ this can be approximated by

$$\tilde{Z}_x(\phi_T, x > 0) \approx \frac{Q}{8\pi} \left[4 \sin^2 \pi \lambda \frac{e^{-\frac{x}{H}}}{(1 - e^{-\frac{x}{H}})^2} \right] \quad (2.74)$$

Integrating this gives

$$\tilde{Z}(\phi_T, x > 0) = C - \frac{QH}{2\pi^2} \sin^2 \pi \lambda \left[\frac{1}{(1 - e^{-\frac{x}{H}})} \right] \quad (2.75)$$

To solve for the constant of integration, C, we note that the perturbation at infinity is twice that at the disc. This is a common property of actuator disks.

$$\frac{\tilde{Z}}{H}(\phi_T, \infty) = 2 \left(\lambda - \frac{\delta}{H} \right) \quad (2.76)$$

Since we know what δ/H equals from equation (2.50), we can solve for the perturbation of the streamline that passes through the blade tip.

$$\frac{\tilde{Z}}{H}(\phi_T, x > 0) = \frac{Q}{2} \left\{ \lambda(1 - \lambda) + \left(\frac{\sin \pi \lambda}{\pi} \right)^2 \left[1 - \frac{1}{(1 - e^{-\frac{x}{H}})} \right] \right\} \quad (2.77)$$

We can now solve for the streamline by adding $1 - \lambda$ to the perturbation.

$$\frac{Z}{H}(\phi_T, x) = 1 - \lambda + \frac{\tilde{Z}}{H} \quad (2.78)$$

Another property of interest is the tip loss. To find it, we first calculate the power per unit depth which is given by

$$P = \int (h_{t_1} - h_{t_3}) d\dot{m} \quad (2.79)$$

With the help of Euler's turbine equation and the substitution

$$d\dot{m} = \rho d\psi \quad (2.80)$$

this becomes

$$P = \rho U \int_0^{\psi_T} [C_x (\tan \alpha_2 + \tan \beta_3) - U] d\psi \quad (2.81)$$

If we linearize and then make the following substitution

$$\varepsilon = \frac{C_{x_0}}{U} [\tan \alpha_2 + \tan \beta_3] \quad (2.82)$$

and use the non-dimensional form of the stream function we get

$$P = \rho U^2 H C_{x_0} \int_0^{\phi_T} \left(\varepsilon \frac{C_x}{C_{x_0}} - 1 \right) d\phi \quad (2.83)$$

Notice that the free wheeling condition occurs when $\varepsilon=1$. The ratio of the velocities is linearized by

$$\frac{C_x}{C_{x_0}} = 1 - C_{x_0} \tilde{Z}_\psi \quad (2.84)$$

which can be rewritten non-dimensionally as

$$\frac{C_x}{C_{x_0}} = 1 - \frac{\partial}{\partial \phi} \left(\frac{\bar{Z}}{H} \right) \quad (2.85)$$

so the term in the parenthesis of equation (2.83) becomes

$$\varepsilon \frac{C_x}{C_{x_0}} - 1 = \varepsilon - 1 - \varepsilon \frac{\partial}{\partial \phi} \left(\frac{\bar{Z}}{H} \right) \quad (2.86)$$

We now define the work coefficient as

$$\Psi = \frac{P}{\rho U^2 H C_{x_0}} \quad (2.87)$$

and rearrange equation (2.83) to get

$$\Psi = \int_0^{\phi_T} \left[\varepsilon - 1 - \varepsilon \frac{\partial}{\partial \phi} \left(\frac{\bar{Z}}{H} \right) \right] d\phi \quad (2.88)$$

Integration yields

$$\Psi = (\varepsilon - 1) \phi_T - \varepsilon \left(\frac{\tilde{Z}_T}{H} \right) \quad (2.89)$$

and since we know what the blade tip perturbation is from equation (2.31a), this becomes

$$\Psi = (\varepsilon - 1) \phi_T - \varepsilon \sum_{n=1}^{\infty} \alpha_n \sin n\pi \phi_T \quad (2.90)$$

With the help of equations (2.48) and (2.49) this can be rearranged and the tip loss can be calculated. The tip loss is given by

$$\frac{\Psi_o - \Psi}{\Psi_o} = \lambda \left[1 + \frac{\varepsilon}{(\varepsilon - 1)} \frac{Q}{4} (1 - \lambda) \right] \quad (2.91)$$

where Ψ_o is the value of the work coefficient when $\lambda=0$.

2.2.2 Non-linear solution

This solution uses a grid and an iteration technique based on pseudo-time marching to approach the true solution. This technique rearranges the governing equation, multiplies it by a constant Δt , and sets it equal to the residual, which is zero at the correct solution. Finite differences are used to calculate parameter values at grid points. These values are then substituted into the governing equation and multiplied by the constant to update the values. By varying the value of the constant the rate of convergence can be changed. If it is too large the solution diverges, and if it is too small the rate of convergence decreases.

To show how this is done we start by rewriting the governing equation as

$$\nabla^2 \psi - \frac{\partial B_{\perp}}{\partial \psi} = 0 \quad (2.92)$$

and taking a perturbation $\delta\psi$ of $\psi(x,z)$, we wish to calculate the following integral (which would be zero for the correct solution):

$$I = \iint \left(\nabla^2 \psi - \frac{\partial B_{\perp}}{\partial \psi} \right) \delta\psi \, dx \, dz \quad (2.93)$$

We can rearrange this into

$$I = \iint \left[\nabla \cdot (\delta\psi \nabla \psi) - \nabla \psi \cdot \nabla (\delta\psi) - \frac{\partial B_{\perp}}{\partial \psi} \delta\psi \right] dx \, dz \quad (2.94)$$

Now with the help of the divergence theorem we get

$$I = \oint \delta\psi \frac{\partial \psi}{\partial n} \, dl - \iint \left[\delta \left(\frac{1}{2} (\nabla \psi)^2 \right) + \delta B_{\perp}(\psi) \right] dx \, dz \quad (2.95)$$

With the substitutions

$$\frac{\partial \psi}{\partial n} = -C_l \quad (2.96)$$

and

$$(\nabla \psi)^2 = C_l^2 \quad (2.97)$$

this becomes

$$-I = \delta \left\{ \iint \left[\frac{1}{2} C_l^2 + B_\perp(\psi) \right] dx dz \right\} + \oint C_l \delta \psi dl \quad (2.98)$$

Imposing the boundary conditions

- | | |
|-------------------------|----------------------------|
| 1) $\delta \psi = 0$ | at the walls |
| 2) $C_l = 0$ | at $+\infty$ and $-\infty$ |
| 3) $\delta B_\perp = 0$ | upstream |

lets us rewrite the equation for a circuit which encloses all of the upstream channel, up to the disk, and then for one which encloses all of the downstream channel, from the disk down.

UPSTREAM:

$$-I^- = \delta \left(\iint_{\text{up}} \frac{1}{2} C_{\perp}^2 dx dz \right) + \int_0^H C_z (x=0^-) \delta\psi_D dz \quad (2.99a)$$

where we made use of $\delta B_{\perp}^- = 0$

DOWNSTREAM:

$$-I^+ = \delta \left\{ \iint_{\text{down}} \left[\frac{1}{2} C_{\perp}^2 + B_{\perp}(\psi) \right] dx dz \right\} - \int_0^H C_z (x=0^+) \delta\psi_D dz \quad (2.99b)$$

Adding these two equations, combining the upstream and downstream integrals, and setting $I = I^+ + I^-$ we find that equation (2.93) gives

$$\delta \left[\iint_{\text{total}} \left(\frac{1}{2} C_{\perp}^2 + B_{\perp} \right) dx dz \right] = \int_0^H (C_z^+ - C_z^-) \delta\psi_D dz + \iint_{\text{total}} \left(\nabla^2 \psi - \frac{\partial B_{\perp}}{\partial \psi} \right) \delta\psi dx dz \quad (2.100)$$

This says that the functional

$$\iint \left(\frac{1}{2} C_{\perp}^2 + B_{\perp} \right) dx dz$$

is at a minimum at the correct solution, and its functional gradient with respect to the local interior variations $\delta\psi$ of ψ is the residual

$$\nabla^2 \psi - \frac{\partial B_{\perp}}{\partial \psi}$$

and its gradient with respect to variations $\delta\psi_D$ of ψ at the disk is the C_z discontinuity.

This opens the way for a gradient-search procedure to find the solution. At interior points we can update ψ using

$$\delta\psi = \Delta t \left[\nabla^2 \psi - \omega_{\nu}(\psi) \right] \quad (2.101)$$

and for points on the disc we use

$$\delta\psi_D = \Delta t_D \left(C_z^+ - C_z^- \right) \quad (2.102)$$

Normalize the variables using the following

$$\psi/H C_{x_0} \rightarrow \psi$$

$$x/H \rightarrow x$$

$$z/H \rightarrow z$$

$$C_x/C_{x_0} \rightarrow C_x$$

$$C_z/C_{x_0} \rightarrow C_z$$

$$U/C_{x_0} \rightarrow 1/\Phi$$

$$\omega_y/(C_{x_0}/H) \rightarrow \omega_y$$

$$Q \rightarrow Q$$

and restate equation (2.101) in the form of the heat conduction equation (with heat generation represented by $-\omega_y$):

$$\frac{1}{\alpha^2} \frac{\partial \psi}{\partial t} = \nabla^2 \psi - \omega_y(\psi) \quad (2.103)$$

where we use a fake diffusivity of α equal to one, and "time march" with a Δt less than one half the square of the smallest grid size. Next the coordinates are changed from (x,z) to (x,ψ) , and equation (2.103) is rewritten as

$$Z_t = -Z_\psi (\nabla^2 \psi - \omega_y(\psi)) \quad (2.104)$$

Now the equation is discretized and the Δt is brought over to the right hand side. This gives

$$Z_{i,j}^{n+1} = Z_{i,j}^n - Z_\psi \left[\nabla^2 \psi - \omega_y(\psi) \right] \delta t \quad (2.105)$$

where $\omega_y(\psi)$ is given by the normalized version of the right hand side of equation (2.27b) and $\nabla^2\psi$ is given by equation (2.25). The derivatives of Z with respect to the other variables are (to second order in the $\Delta\psi$ and Δx)

$$Z_x = \frac{\frac{h^-}{h^+} Z_{i+1,j} - \frac{h^+}{h^-} Z_{i-1,j}}{h^+ + h^-} + \frac{h^+ - h^-}{h^+ h^-} Z_{i,j} \quad (2.106a)$$

$$Z_\psi = \frac{\frac{k^-}{k^+} Z_{i,j+1} - \frac{k^+}{k^-} Z_{i,j-1}}{k^+ + k^-} + \frac{k^+ - k^-}{k^+ k^-} Z_{i,j} \quad (2.106b)$$

$$Z_{xx} = 2 \frac{\frac{Z_{i+1,j}}{h^+} + \frac{Z_{i-1,j}}{h^-}}{h^+ + h^-} - 2 \frac{Z_{i,j}}{h^+ h^-} \quad (2.106c)$$

$$Z_{\psi\psi} = 2 \frac{\frac{Z_{i,j+1}}{k^+} + \frac{Z_{i,j-1}}{k^-}}{k^+ + k^-} - 2 \frac{Z_{i,j}}{k^+ k^-} \quad (2.106d)$$

$$Z_{x\psi} = \frac{Z_{i+1,j+1} - Z_{i+1,j} - Z_{i,j+1} + Z_{i,j}}{h^+ k^+} \quad (2.106e)$$

where we define

$$h^- = x_i - x_{i-1} \quad (2.107a)$$

$$h^+ = x_{i+1} - x_i \quad (2.107b)$$

$$k^- = \psi_i - \psi_{i-1} \quad (2.107c)$$

$$k^+ = \psi_{i+1} - \psi_i \quad (2.107d)$$

For points along the disc, since the Δx values are taken equal on either side, equation (2.102) is replaced by

$$(Z_t)_{x=0} = \frac{1}{2} (Z_x^+ - Z_x^-) \quad (2.108)$$

which can be rewritten

$$Z_{0,j}^{n+1} = Z_{0,j}^n + \frac{1}{2} \left(\frac{Z_{1,j} - Z_{0,j}}{x_1} - \frac{Z_{0,j} - Z_{-1,j}}{x_1} \right) \delta t \quad (2.109)$$

and if we use a $(\delta t)/(\Delta x) = 1/2$ then this becomes

$$Z_{0,j}^{n+1} = \frac{1}{2} Z_{0,j}^n + \frac{1}{4} (Z_{i,j} + Z_{-i,j}) \quad (2.110)$$

To calculate $Z_{i,j}$ along ψ_T we first integrate $\nabla^2 \psi$ across the velocity discontinuity. Because Z_x is continuous, Z_ψ has a discontinuity, and $Z_{\psi\psi}$ has a delta function, the only term in equation (2.25) that remains after integration is the last one.

$$\int_{-}^{+} - (1 + Z_x^2) \frac{Z_{\psi\psi}}{Z_\psi^3} d\psi = \frac{1 + Z_x^2}{2} \left(\frac{1}{Z_\psi^{+2}} - \frac{1}{Z_\psi^{-2}} \right) \quad (2.111)$$

This must be equal to the integral of the vorticity across the velocity discontinuity:

$$\int_{-}^{+} \omega_y d\psi = \frac{C_x^-}{\Phi} \tan \alpha_2 - \frac{1}{2} \left(\frac{1}{\Phi^2} - C_x^{-2} \tan^2 \beta_3 \right) - \frac{1}{2} C_x^{+2} \tan^2 \alpha_2 = \frac{Q}{2} \quad (2.112)$$

where Q is the same quantity as was introduced before (Eq. 2.41)

$$(1 + Z_x^2) \left(\frac{1}{Z_\psi^{+2}} - \frac{1}{Z_\psi^{-2}} \right) = Q \quad (2.113)$$

Using one-sided differences for Z_ψ , with equal $\Delta\psi$ on both sides, allows us to rewrite this as

$$(1 + Z_x^2) (\Delta\psi)^2 \left[\frac{1}{(Z_{i,j} - Z_{i,j-1})^2} - \frac{1}{(Z_{i,j+1} - Z_{i,j})^2} \right] = Q \quad (2.114)$$

This can't be solved for $Z_{i,j}$ explicitly so it is iterated using the following form.

$$Z_{i,j} = \frac{Z_{i,j+1} + Z_{i,j-1}}{2} + \frac{Q (Z_{i,j+1} - Z_{i,j})^2 (Z_{i,j} - Z_{i,j-1})^2}{2 (\Delta\psi)^2 (Z_{i,j-1} - Z_{i,j+1}) (1 + Z_x^2)} \quad (2.115)$$

We can now iterate through the (x, ψ) grid to calculate the values of $Z_{i,j}$.

2.3 Modifications

After the initial theory was complete it was noticed that the calculated flow perturbations were larger than expected. Two modifications were made to make the model more realistic. The first was to change the theory to allow compressible flow. This had only a small effect on the flow perturbations. The second modification took into account the theory of retained lift which was put forth by Lakshminarayana¹⁰. This can have a substantial effect on the flow perturbation and can bring it to a level similar to that observed in experiments.

2.3.1 Compressible Flow

To approximate a real turbine the variable density model uses constant axial velocities and deals with the density change by increasing the channel height through the actuator disc (Fig 2.5). This changes two of the matching conditions at the disc. First the flow perturbation is amplified by the density ratio.

$$\left(\tilde{Z}\right)_{x=0+} = \frac{\rho_1}{\rho_3} \left(\tilde{Z}\right)_{x=0-} \quad (2.116)$$

Second the derivative of the flow perturbation with respect to ψ is also amplified by the density ratio.

$$\left(\tilde{Z}_\psi\right)_{x=0+} = \frac{\rho_1}{\rho_3} \left(\tilde{Z}_\psi\right)_{x=0-} \quad (2.117)$$

The derivative of the flow perturbation with respect to x remains the same since the axial velocity is constant across the actuator disc. Therefore the solutions to the constant density model are modified to become

$$\tilde{Z} = H \sum_{n=1}^{\infty} \alpha_n e^{\frac{n\pi x}{H}} \sin n\pi \frac{\psi}{\psi_{top}} \quad x < 0 \quad (2.118a)$$

$$\tilde{Z} = H \frac{\rho_1}{\rho_3} \sum_{n=1}^{\infty} \alpha_n \left(2 - e^{-\frac{\rho_3}{\rho_1} \frac{n\pi x}{H}}\right) \sin n\pi \frac{\psi}{\psi_{top}} \quad x > 0 \quad (2.118b)$$

To find the constants α_n , we need to find the vorticity created by the actuator disc. For compressible flow, we begin the derivation with the enthalpy equation

$$H = h + \frac{C^2}{2} \quad (2.119)$$

where H is the total enthalpy, h is the static enthalpy and C is the velocity. We define the perpendicular total enthalpy as

$$H_{\perp} = H - \frac{C_y^2}{2} \quad (2.120)$$

where C_y is the y -component of the velocity. Since there are no variations in the y -direction the relationship

$$\vec{\omega} \times \vec{C} = -\nabla H \quad (2.121)$$

can be written

$$\omega_z C_x - \omega_x C_z = 0 \quad (2.122a)$$

$$\omega_y C_z - \omega_z C_y = -\frac{\partial H_\perp}{\partial x} - C_y \left(\frac{\partial C_y}{\partial x} \right) \quad (2.122b)$$

$$\omega_x C_y - \omega_y C_x = -\frac{\partial H_\perp}{\partial z} - C_y \left(\frac{\partial C_y}{\partial z} \right) \quad (2.122c)$$

and the vorticity equations simplify to

$$\omega_x = - \left(\frac{\partial C_y}{\partial z} \right) \quad (2.123a)$$

$$\omega_y = \left(\frac{\partial C_x}{\partial z} \right) - \left(\frac{\partial C_z}{\partial x} \right) \quad (2.123b)$$

$$\omega_z = \left(\frac{\partial C_y}{\partial x} \right) \quad (2.123c)$$

Inserting equations (2.123a) and (2.123c) into equations (2.122b) and (2.122c) gives the result

$$\omega_y = -\frac{1}{C_z} \left(\frac{\partial H_\perp}{\partial x} \right) \quad (2.124a)$$

$$\omega_y = \frac{1}{C_x} \left(\frac{\partial H_\perp}{\partial z} \right) \quad (2.124b)$$

The stream function is used to satisfy continuity. For the variable density case this gives

$$C_x = \frac{\rho_1}{\rho_3} \left(\frac{\partial \psi}{\partial z} \right) \quad (2.125a)$$

$$C_z = -\frac{\rho_1}{\rho_3} \left(\frac{\partial \psi}{\partial x} \right) \quad (2.125b)$$

Combining equations (2.124a) and (2.124b) with (2.125a) and (2.125b) give us the relationship needed for the downstream governing equation.

$$\omega_y = \frac{\rho_3}{\rho_1} \left(\frac{\partial H_{\perp}}{\partial \psi} \right) \quad (2.126)$$

Now we have to manipulate this expression of the vorticity into a useful form. To do this we take the downstream perpendicular total enthalpy

$$H_{\perp} = h_3 + \frac{C_{x3}^2}{2} + \frac{C_{z3}^2}{2} \quad (2.127)$$

and expand it into

$$H_{\perp 3} = h_1 + \left(\frac{C_{x_1}^2 + C_{z_1}^2}{2} \right) - (h_1 - h_3) - \left(\frac{C_{x_1}^2 - C_{x_3}^2}{2} \right) \quad (2.128)$$

which simplifies to

$$H_{\perp 3} = H_{\perp 1} - (h_1 - h_3) \quad (2.129)$$

Because the upstream flow is uniform and unperturbed the perpendicular total enthalpy doesn't vary with the stream function. Therefore, taking the derivative of the downstream perpendicular total enthalpy gives

$$\frac{\partial H_{\perp 3}}{\partial \psi} = - \frac{\partial}{\partial \psi} (h_1 - h_3) \quad (2.130)$$

From Euler's turbine equation we can find the static enthalpy drop for the blade region.

$$h_1 - h_3 = UC_x \tan \alpha_2 - \frac{1}{2} \left(U^2 - C_x^2 \tan^2 \beta_3 \right) \quad \psi < \psi_T \quad (2.131)$$

Substituting this into equation (2.130), changing variables with the help of equation (2.19), and

taking the derivative with respect to C_x gives

$$\frac{\partial H_{\perp 3}}{\partial \psi} = - \left[\frac{U}{C_x} \tan \alpha_2 + \tan^2 \beta_3 \right] \left(\frac{\partial C_x}{\partial Z} \right)_{x=0} \quad \psi < \psi_T \quad (2.132)$$

Now we have to find the static enthalpy drop for the gap region. We start by noting

$$H_{\perp 3} = H_{\perp 1} - \frac{C_x^2}{2} \quad \psi > \psi_T \quad (2.133)$$

which is equal to

$$H_{\perp 3} = H_{\perp 1} - \frac{C_x^2}{2} \tan^2 \alpha_2 \quad \psi > \psi_T \quad (2.134)$$

Taking the derivative of this with respect to the stream function gives

$$\frac{\partial H_{\perp 3}}{\partial \psi} = - \left[\tan^2 \alpha_2 \right] \left(\frac{\partial C_x}{\partial Z} \right)_{x=0} \quad \psi > \psi_T \quad (2.135)$$

Substituting the blade and gap expressions into the vorticity equation (2.126) gives

BLADE:

$$\omega_y = -\frac{\rho_3}{\rho_1} \left[\frac{U}{C_x} \tan \alpha_2 + \tan^2 \beta_3 \right] \left(\frac{\partial C_x}{\partial Z} \right)_{x=0} \quad (2.136a)$$

GAP:

$$\omega_y = -\frac{\rho_3}{\rho_1} \left[\tan^2 \alpha_2 \right] \left(\frac{\partial C_x}{\partial Z} \right)_{x=0} \quad (2.136b)$$

Now we need to calculate the vorticity produced by the shear layer. We start by finding the integral of the vorticity across the blade tip. This is given by

$$\int \omega_y d\psi = \frac{\rho_3}{\rho_1} (H_{\perp_3}^+ - H_{\perp_3}^-) \quad (2.137)$$

Plugging in the values for $H_{\perp_3}^+$ and $H_{\perp_3}^-$ which we just found and linearizing C_x gives

$$\omega_y = \frac{\rho_3}{\rho_1} \left\{ UC_x \tan \alpha_2 + \frac{1}{2} \left[C_x^2 \tan^2 \beta_3 - C_x^2 \tan^2 \alpha_2 - U^2 \right] \right\} \delta(\psi - \psi_T) \quad (2.138)$$

Substituting equations (2.136a), (2.136b) and (2.138) into (2.5) gives the governing equation for the downstream region. From this point on the solution is the same as the incompressible problem except the vorticities are multiplied by the density ratio. This means the constants α_n have the same form as the constant density case (2.48) except Q is now defined as the solution

to the quadratic equation

$$\begin{aligned}
 & Q^2 \left[\frac{\lambda^2}{16} \tan^2 \beta_3 - \frac{(1-\lambda)^2}{16} \tan^2 \alpha_2 \right] + \\
 & Q \left[-\frac{(1-\lambda)}{2} \tan^2 \alpha_2 - \frac{\lambda}{2\Phi} \tan \alpha_2 - \frac{\lambda}{2} \tan^2 \beta_3 - \frac{\rho_1}{\rho_3} \right] + \\
 & \left[\frac{2}{\Phi} \tan \alpha_2 - \frac{1}{\Phi^2} + \tan^2 \beta_3 - \tan^2 \alpha_2 \right] = 0
 \end{aligned} \tag{2.139}$$

where the density ratio is either given directly or calculated from a given blade Mach number.

2.3.2 Retained Lift

The retained lift theory assumes that the flow passing through the gap does some work on the blade. Previously we had the pressure drop or total enthalpy drop across the gap equal zero. For the retained lift theory, the drop in pressure or total enthalpy across the gap is a fraction of that across the blade. If we define K as the ratio of the total enthalpy drops across the gap and blade, then we can write

$$K = \frac{\frac{2}{\Phi} \left(\frac{C_x^-}{C_{x_o}} \right) \tan \alpha_2 - \frac{1}{\Phi^2} + \left(\frac{C_x^-}{C_{x_o}} \right)^2 \tan^2 \beta_4 - \left(\frac{C_x^+}{C_{x_o}} \right)^2 \tan^2 \alpha_2}{\frac{2}{\Phi} \left(\frac{C_x^-}{C_{x_o}} \right) \tan \alpha_2 - \frac{1}{\Phi^2} + \left(\frac{C_x^-}{C_{x_o}} \right)^2 \tan^2 \beta_3 - \left(\frac{C_x^+}{C_{x_o}} \right)^2 \tan^2 \alpha_2} \tag{2.140}$$

where β_4 is a fictitious blade angle that would appear in the gap region to extract work from the fluid. Note that when the fictitious blade is free-wheeling this corresponds to $K=0$, and no work is done in the gap region. This occurs when

$$\left(\frac{C_x^-}{C_{x_o}} \right)^2 \tan^2 \beta_4 = \frac{1}{\Phi^2} - \frac{2}{\Phi} \left(\frac{C_x^-}{C_{x_o}} \right) \tan \alpha_2 + \left(\frac{C_x^+}{C_{x_o}} \right)^2 \tan^2 \alpha_2 \tag{2.141}$$

This corresponds to what we had previously for the gap region. If $K=1$ then $\beta_4=\beta_3$ and the enthalpy drop across the gap is the same as that across the blade. Since no shear layer forms, the flow is unperturbed.

The solution to the retained lift problem has the same form as the previous linear solutions. The only difference is how Q is defined. Since Q is a measure of the strength of the shear layer, it is proportional to the difference in pressure or total enthalpy drop across the gap and the blade. So for the constant density case Q is

$$Q = \left(\frac{C_x^-}{C_{x_0}} \right)^2 (\tan^2 \beta_3 - \tan^2 \beta_4) \quad (2.142)$$

However, both the blade velocity and the fictitious blade angle are functions of Q , so to solve for Q an iteration is needed. For the variable density case Q is

$$Q = \frac{\rho_3}{\rho_1} \left(\frac{C_x^-}{C_{x_0}} \right)^2 (\tan^2 \beta_3 - \tan^2 \beta_4) \quad (2.143)$$

and again an iteration is needed to solve for Q . By controlling the value of K , the values of δ/H and the tip loss can be kept to realistic values.

To support the retained lift theory we note that some of the fluid that exits the gap has actually passed through part of the bladed region and then flowed over the blade tip (Fig 2.6). This fluid has done some work on the blade. By introducing the fictitious blade in the gap we can account for this work.

CHAPTER 3

RESULTS

To see how well the two-level velocity model approximates the non-linear model we compare their axial and radial velocities. This is done for a series of different turbines having reactions that range from .10 to .975. All turbines are at the design point of no exit swirl, which is given by

$$\tan \beta_3 = \frac{1}{\Phi} \quad (3.10)$$

For this analysis, Φ and $\tan \beta_3$ are held constant at .5 and 2, and the reaction is varied by changing $\tan \alpha_2$ using

$$R = \frac{1}{2} [3 - \Phi (\tan \alpha_2 + \tan \beta_3)] \quad (3.2)$$

For reactions of zero and one, the pressure drop across the rotor is zero because these represent the impulse turbine and free-wheeling conditions. Since no pressure drop occurs, $Q=0$ and the flow is unperturbed. The two-level velocity model and the non-linear model converge to the same solution of no flow perturbation at these points. For reactions between zero and one, $Q>0$. The two-level model approximates the non-linear model fairly well, but it gets noticeably worse at large values of Q . This is shown in Figures 3.1-3.16, where the non-linear solution used a 16x32 grid that covered two blade spans upstream and downstream of the actuator disk. Note that the

given Q is for the two-level velocity model.

To show that sufficient grid points were used to generate an accurate solution, a 16X32 grid was compared to a 24X48 grid. When this comparison was performed for a reaction value of .80 (where Q had the greatest observed value for the two-level velocity model) the differences between the calculated velocities were relatively small. The grid points common to both grids and their respective calculated velocities can be seen in Table 3.1.

To demonstrate the effect of reaction on the tip loss to gap size ratio and the gap size, λ was held constant at .10 while the reaction was varied from zero to one. At reactions of zero and one, both the tip loss to gap size ratio and the gap size were equal to λ because the flow is unperturbed. At reactions from .70 to .80 the effect on the tip loss to gap size ratio and the gap size is quite large, because Q is relatively large. This is shown in Figures 3.17 and 3.18.

The effect of λ on the jet velocity is relatively small for a given turbine. This can be seen in Fig. 3.19. As λ increases more flow is lost to the gap causing the blade velocity to fall. This agrees with experimental data which shows the jet velocity remains approximately constant.

To show the effects of turbine operation at off-design conditions the turbine blade angles were held constant at $\tan\alpha_2=2$ and $\tan\beta_3=.2$, and the flow coefficient was varied from .46 to .54. Therefore the turbine would only operate at design when $\Phi=.5$. By holding the gap size, δ/H , constant the tip loss to gap size ratio can be found as a function of Φ . Similarly by holding the work coefficient, Ψ , constant the tip loss to gap size ratio can be found as a function of Φ . This is shown in Fig. 3.20 for different values of gap size and work coefficient. As Φ increases, both the tip loss to gap size ratio and the work coefficient increase for a given gap size. This is because for small values of Φ the rotor is almost unloaded. As Φ increases, so does the turbine loading and the work coefficient. The fluid sees the rotor as a resistance to the flow and tries to avoid it by moving toward the gap. Therefore as the turbine loading increases so does the tip loss to gap size ratio.

The tip loss to gap size ratio for real turbines is generally in the 1.2 to 1.8 range. Since the

linear model produces values between 3.0 and 4.0, two modifications were made to the theory. The first was to allow compressible flow. This reduced the tip loss to gap size ratio but not significantly. The second modification used the theory of retained lift which allows the fluid in the gap to do some work. This produces reasonable tip loss to gap size ratios. To demonstrate the effects of these modifications, the flow coefficient versus the tip loss to gap size ratio was plotted for a constant gap size of .05 for four different cases. This is shown in Fig. 3.21 where K is defined by equation (2.140), and d_3/d_1 is the density ratio. By combining the retained lift theory and variable density the tip loss to gap size ratio can be significantly improved.

CHAPTER 4**RECOMMENDATIONS**

To gain more understanding into the gap's effect on the flow perturbations, three recommendations are made. First, accurate experimental data is needed to verify the theory of constant axial velocities for the gap and blade regions. Second, a means of determining the value of K for the retained lift theory is needed. Lastly, a theory that takes into account variable gap size is required. Since real rotors are generally slightly off-center, they produce variable gap sizes that can affect the flow field upstream of the rotor. It is felt that a three dimensional actuator disk model is needed to simulate this flow field.

REFERENCES

1. Childs, D. "The Space Shuttle Main Engine High Pressure Fuel Turbopump Instability Problem," ASME Trans. Journal of Engineering for Power, Jan. 1978, pp. 48-57.
2. Ehrich, F., and Childs, S.D., "Self-Excited Vibrations in High-Performance Turbomachinery," Mechanical Engineering, May 1984, pp. 66-79.
3. Kimball, A.L., Jr., "Internal Friction Theory of Shaft Whirling," General Electric Review, Vol. 27, April 1924, pp. 244-251.
4. Hartog, J.P., "Mechanical Vibrations", 4th ed., McGraw-Hill Book Company, Inc., New York, 1956.
5. Newkirk, B.L., and Taylor, H.D., "Shaft Whipping Due to Oil Action in Journal Bearing", General Electric Review, Vol. 28, 1925, pp. 559-568.
6. Iwatsubo, T., "Evaluation of Instability Forces of Labyrinth Seals in Turbines or Compressors," NASA C.D. 2133, 1980, pp. 139-169.
7. Alford, J.S., "Protecting Turbomachinery from Self-Excited Rotor Whirl", Journal of Engineering for Power, Oct. 1965.
8. Thomas, H.J., "Unstable Oscillations of Turbine Rotors Due to Steam Leakage in the Clearance of the Sealing Glands and the Buckets", Bulletin Scientifique, A.J.M., Vol. 71, 1958.
9. Y. Qiu, M. Martinez-Sanchez, and E.M. Greltzer, "The Prediction of Destabilizing Blade-Tip Forces For Shrouded and Unshrouded Turbines," presented at the Symposium on Instability of Rotating Machinery, Carson City, NV, June 1985.
10. Lakshminarayana, B. "Tip Clearance Effects in Turbomachines", Lecture 4, Pennsylvania State University, April 14-18, 1986.
11. Horlock, J.H., "Actuator Disk Theory", McGraw-Hill International Book Company, Inc., New York, p. 78.

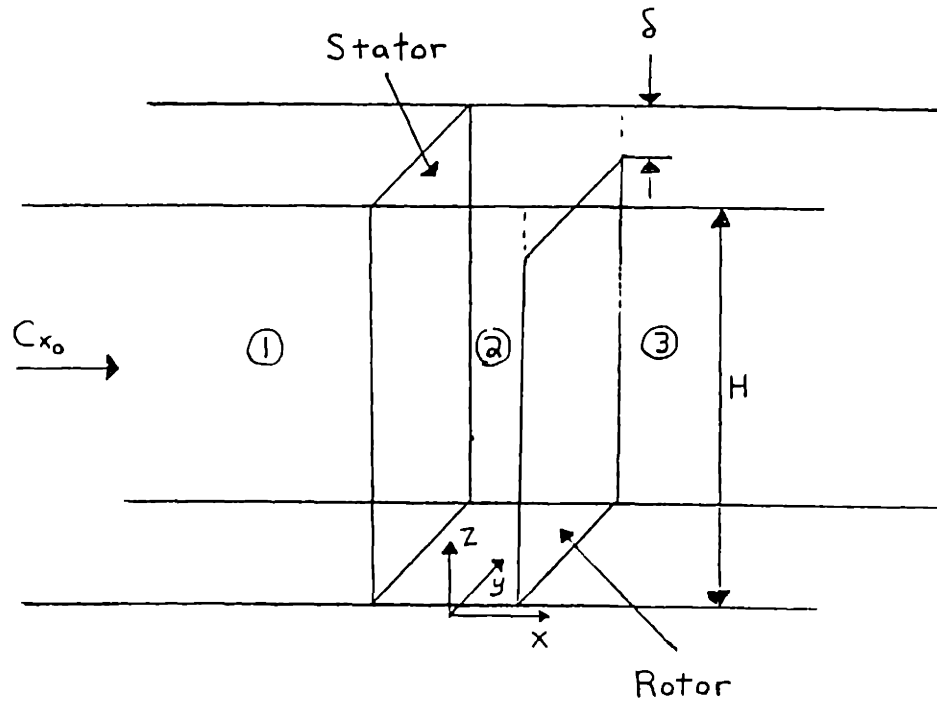


Fig. 2.1 Channel flow with constant blade-tip clearance

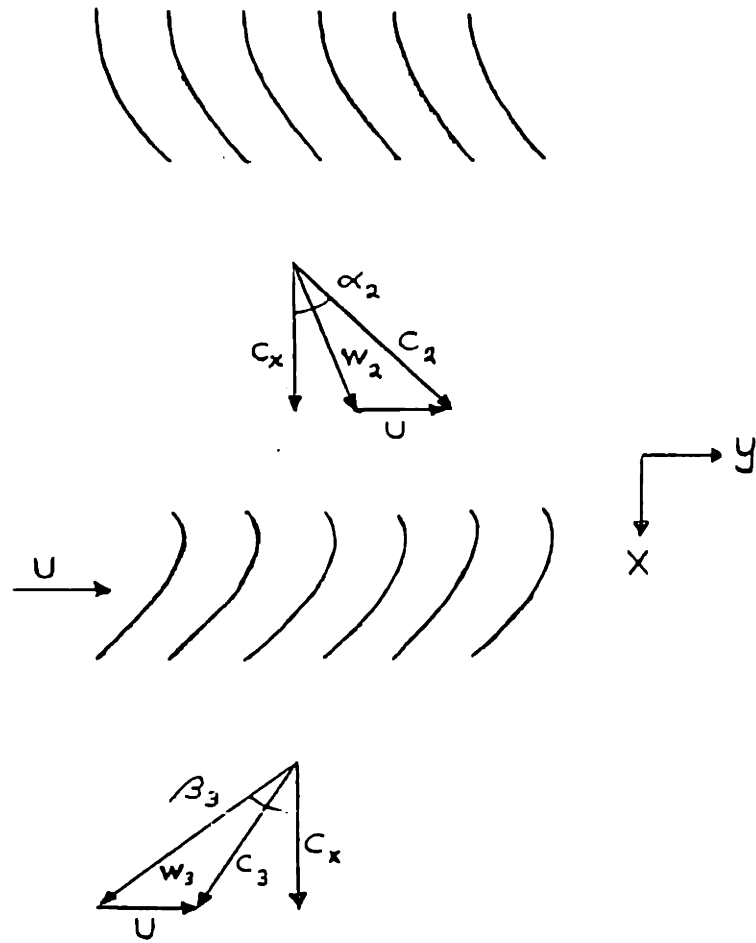


Fig. 2.2 Velocity triangles

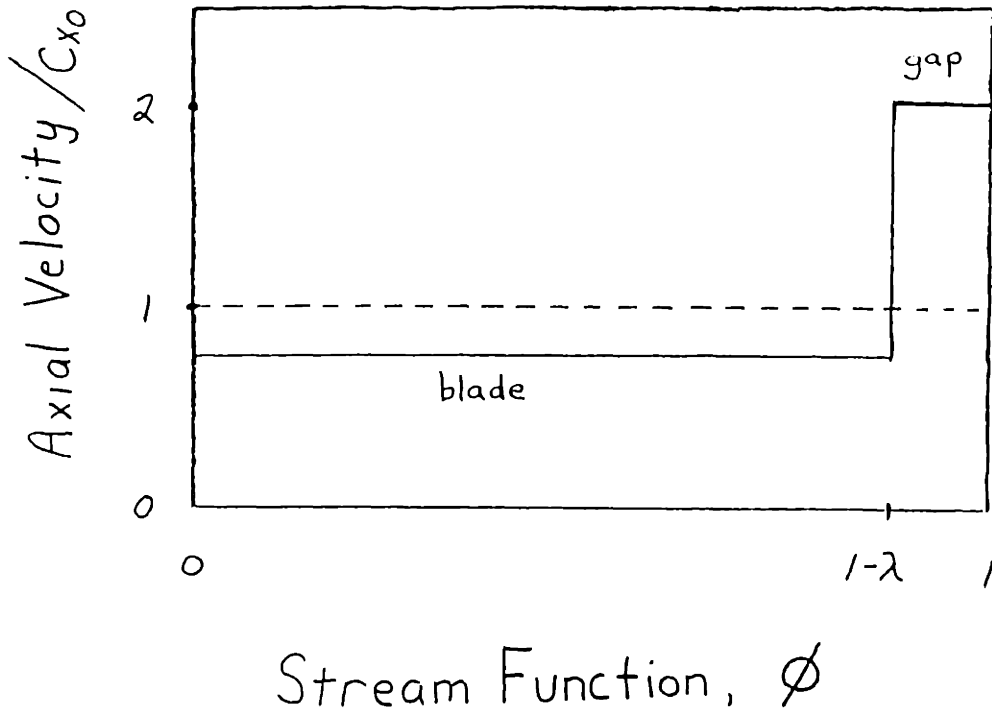


Fig. 2.3 Constant axial velocities

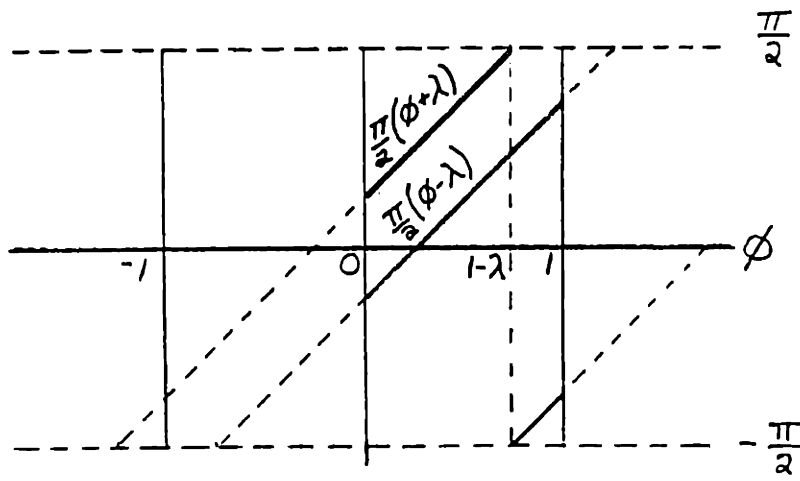


Fig. 2.4 Jump caused by arctan

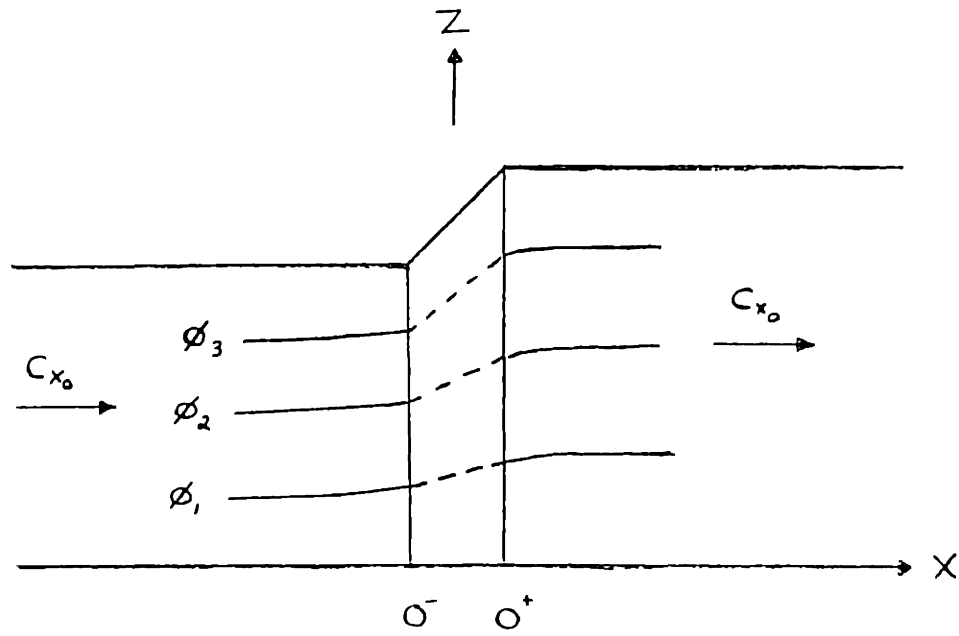


Fig. 2.5 Channel flow for variable density case

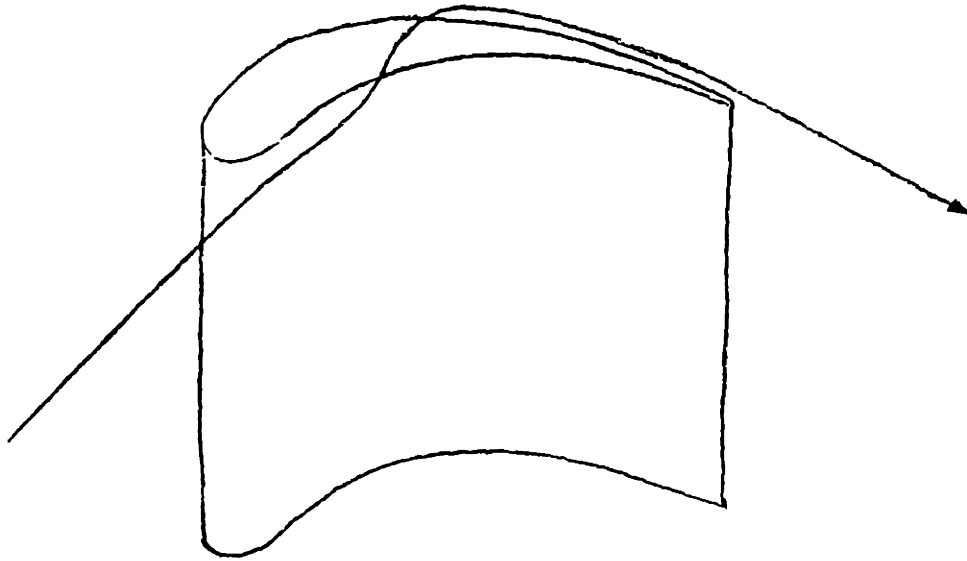


Fig. 2.6 Gap fluid that does some work on the rotor

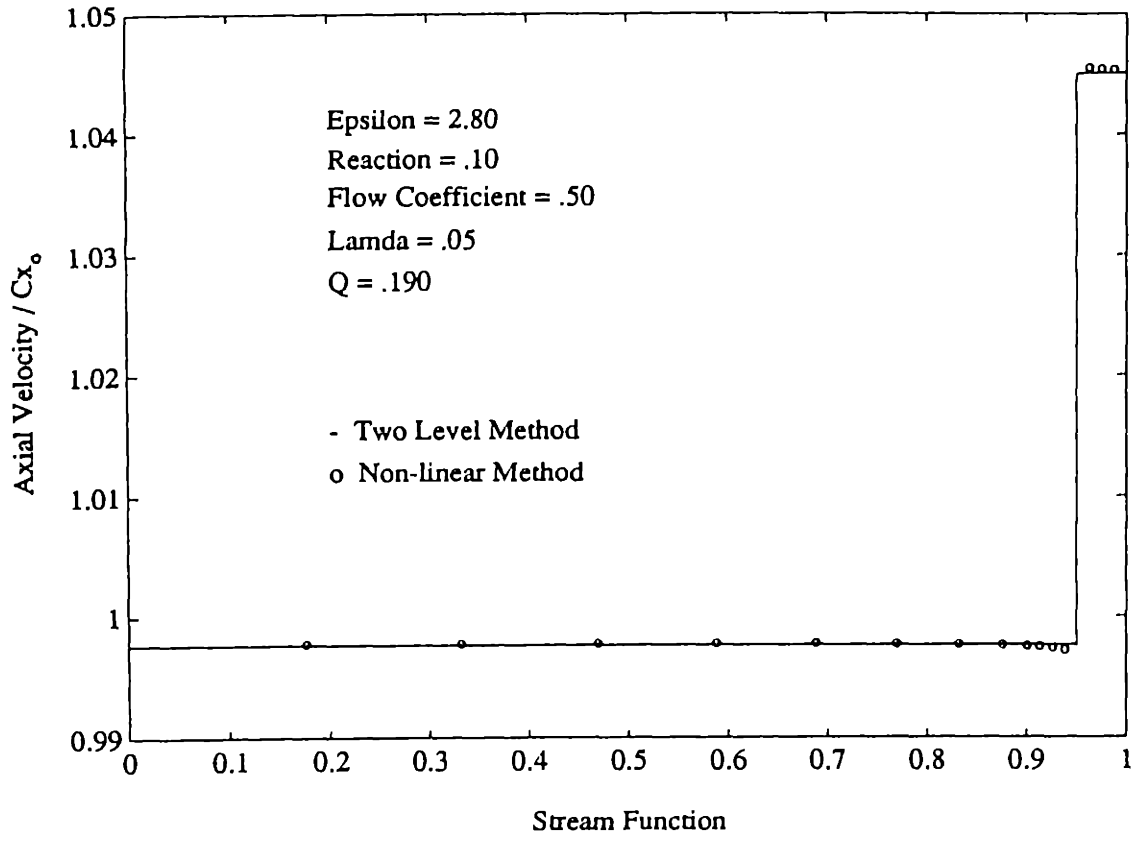


Fig. 3.1

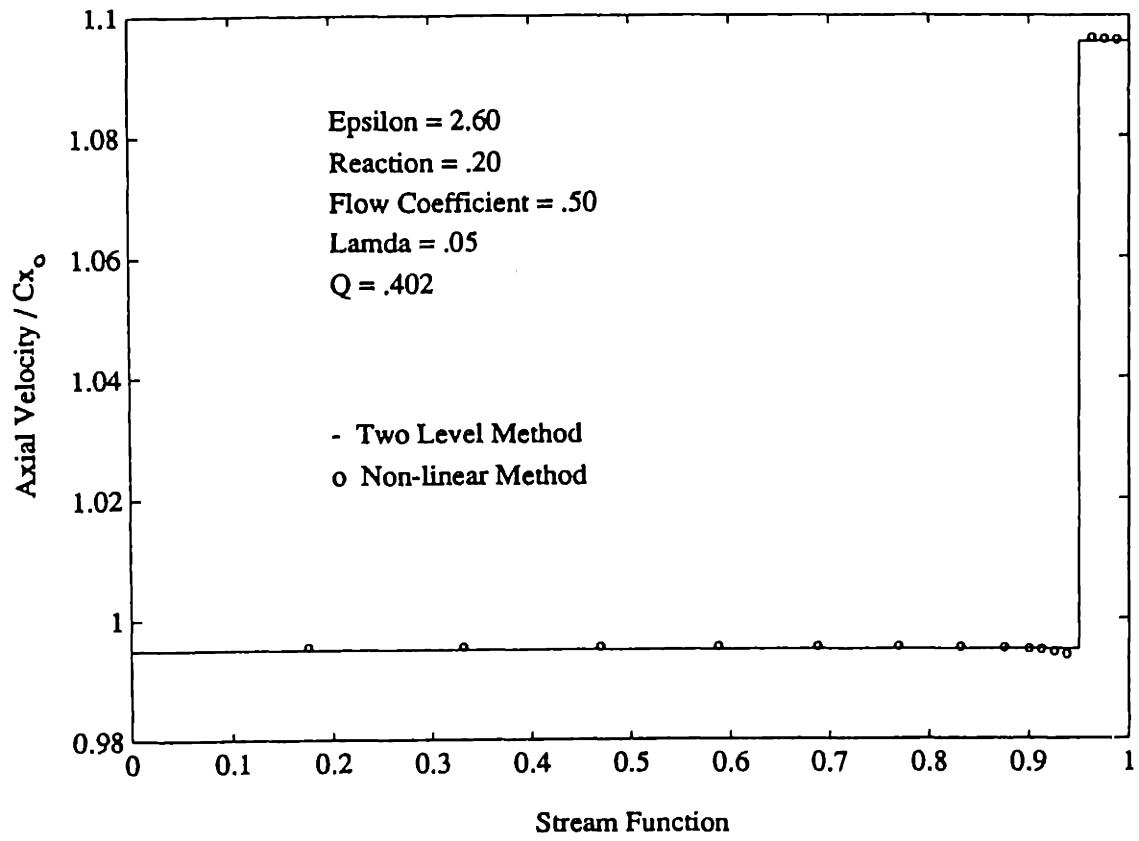


Fig. 3.2

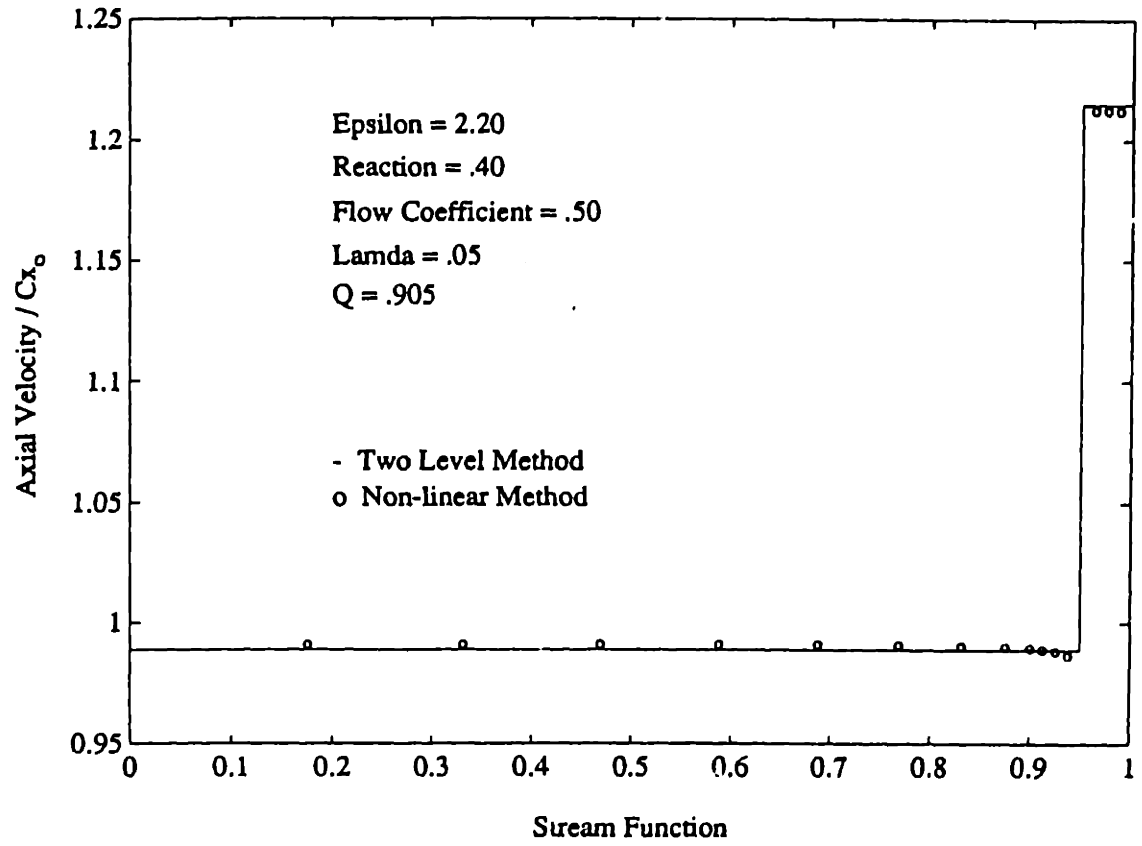


Fig. 3.3

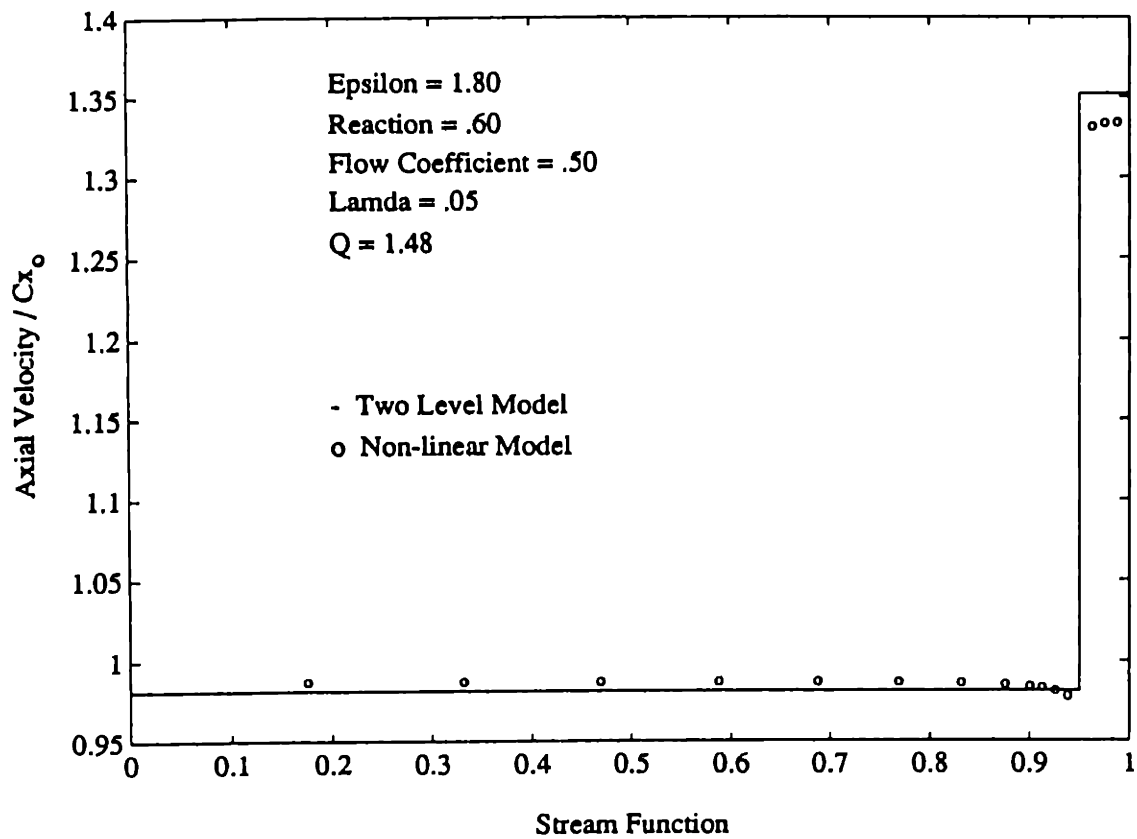


Fig. 3.4

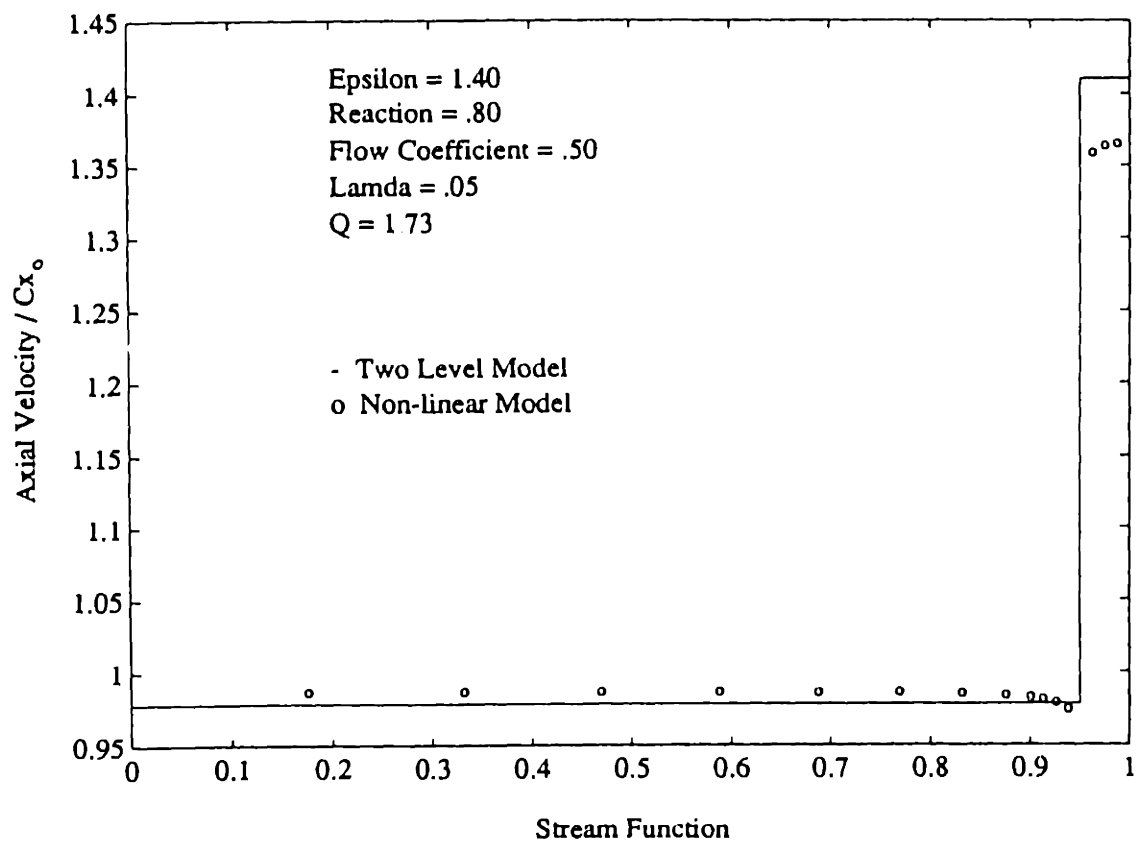


Fig. 3.5

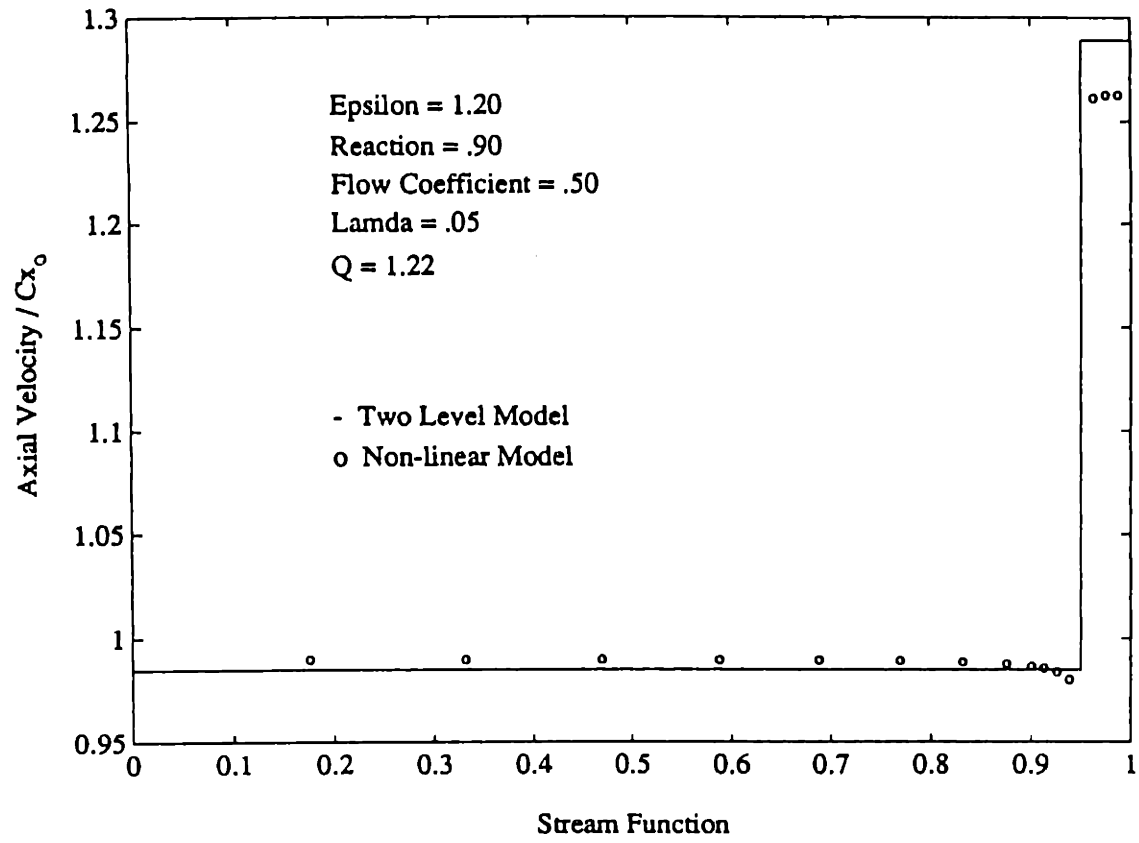


Fig. 3.6

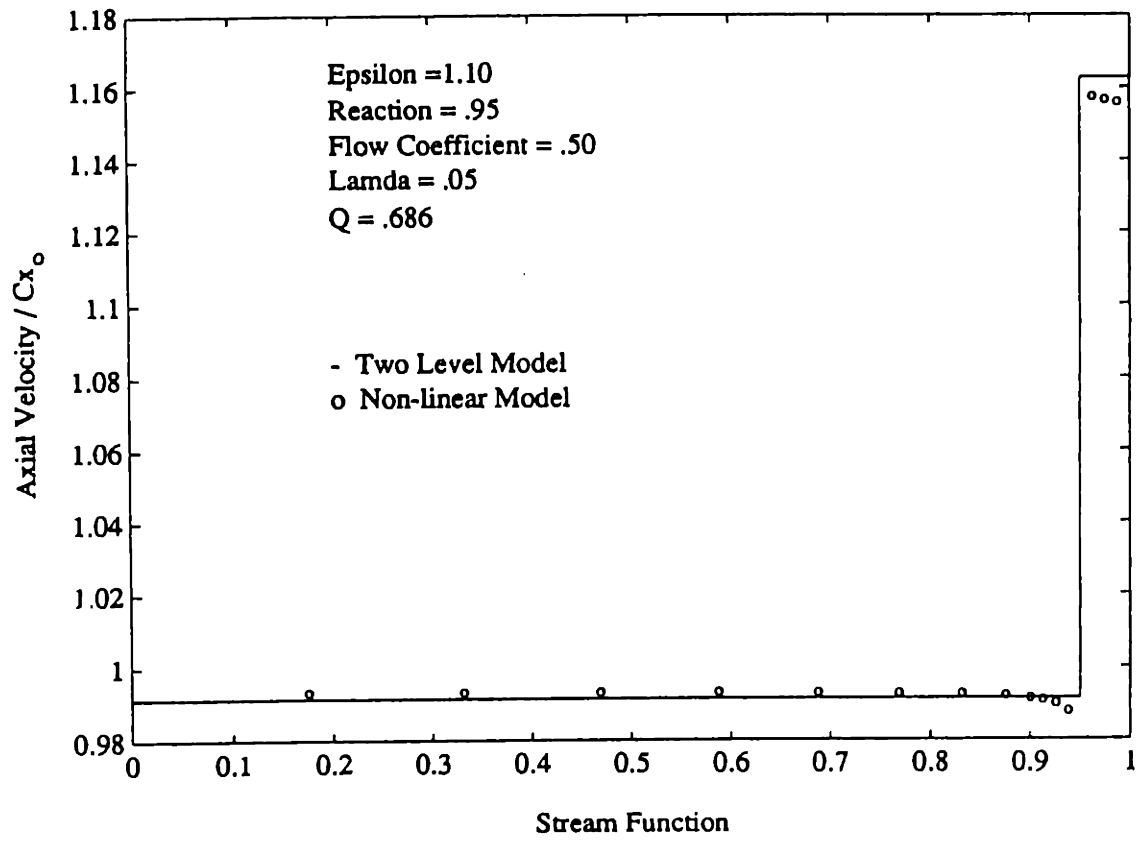


Fig. 3.7

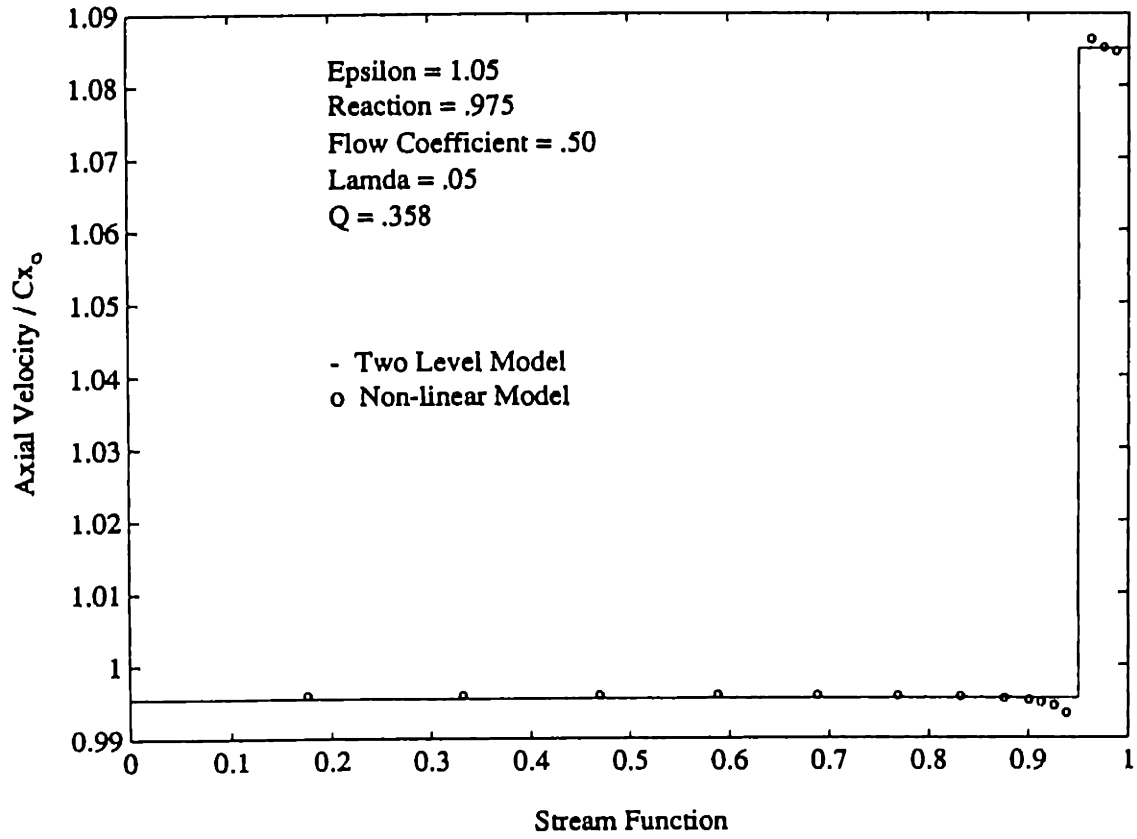


Fig. 3.8

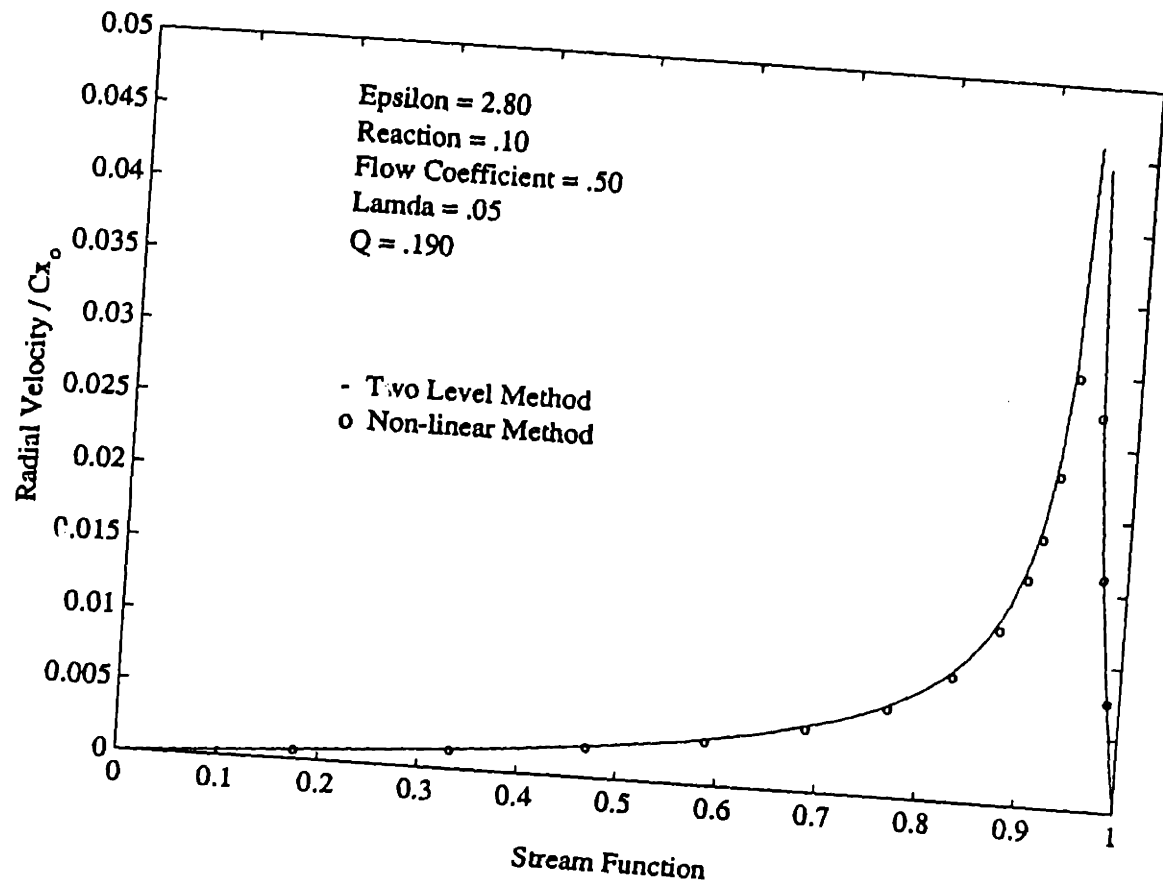


Fig. 3.9

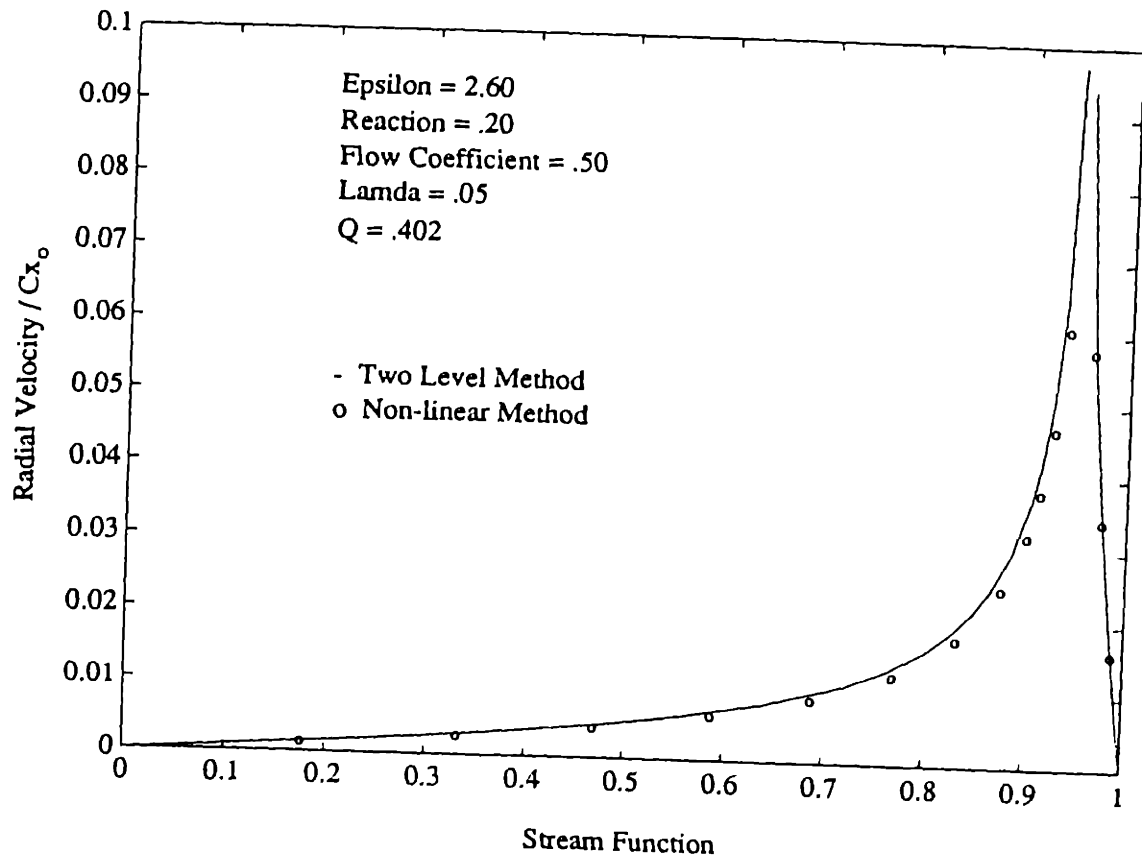


Fig. 3.10

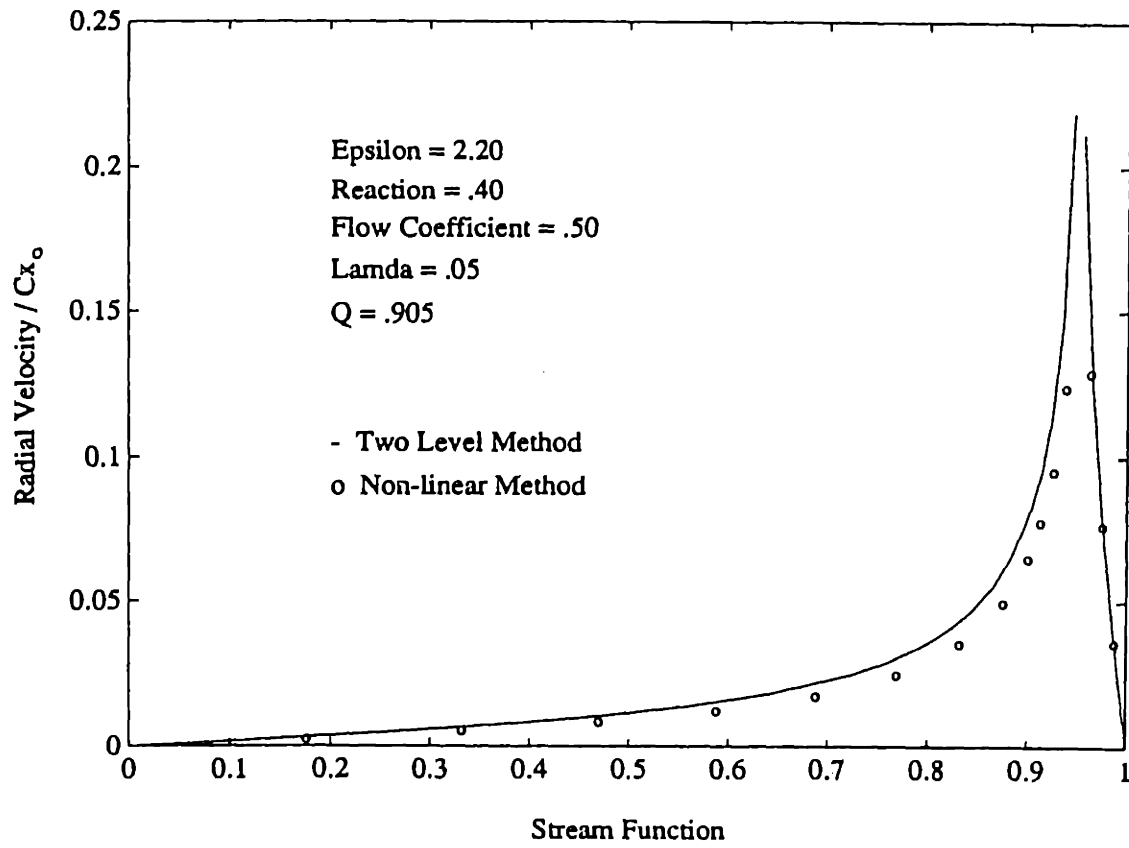


Fig. 3.11

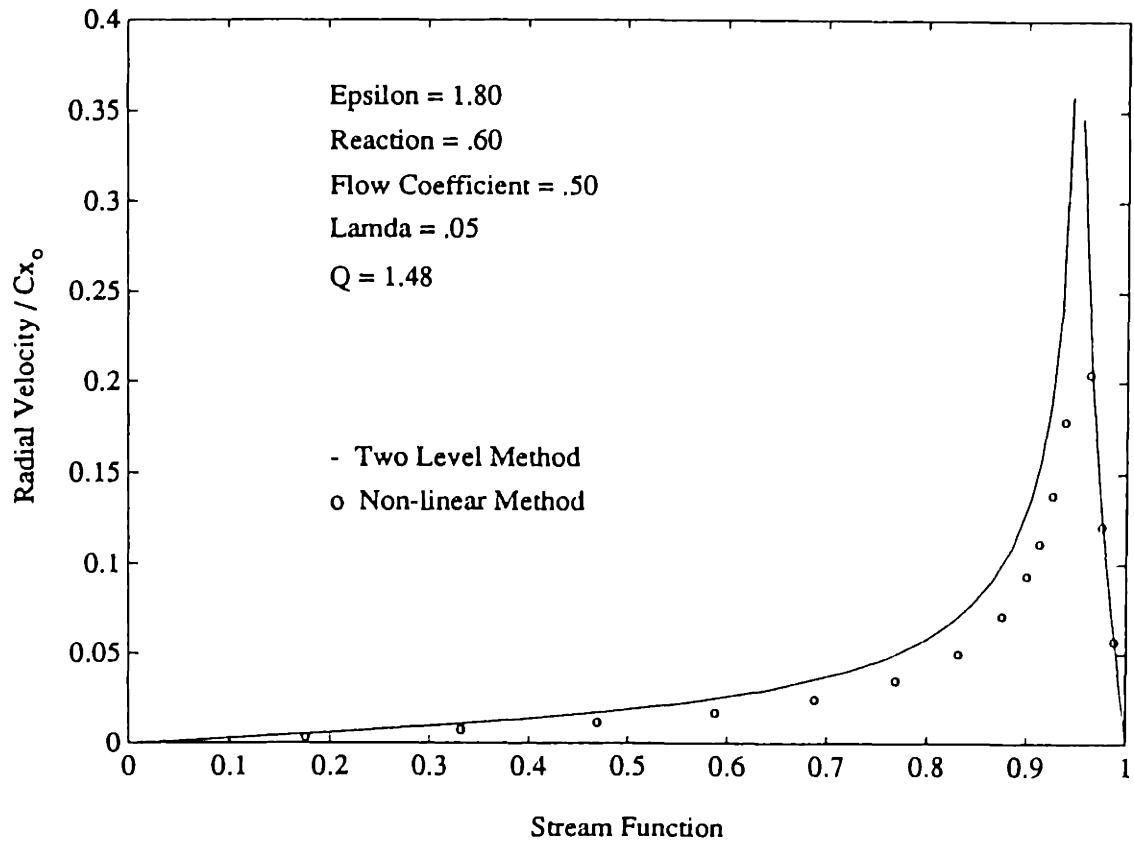


Fig. 3.12

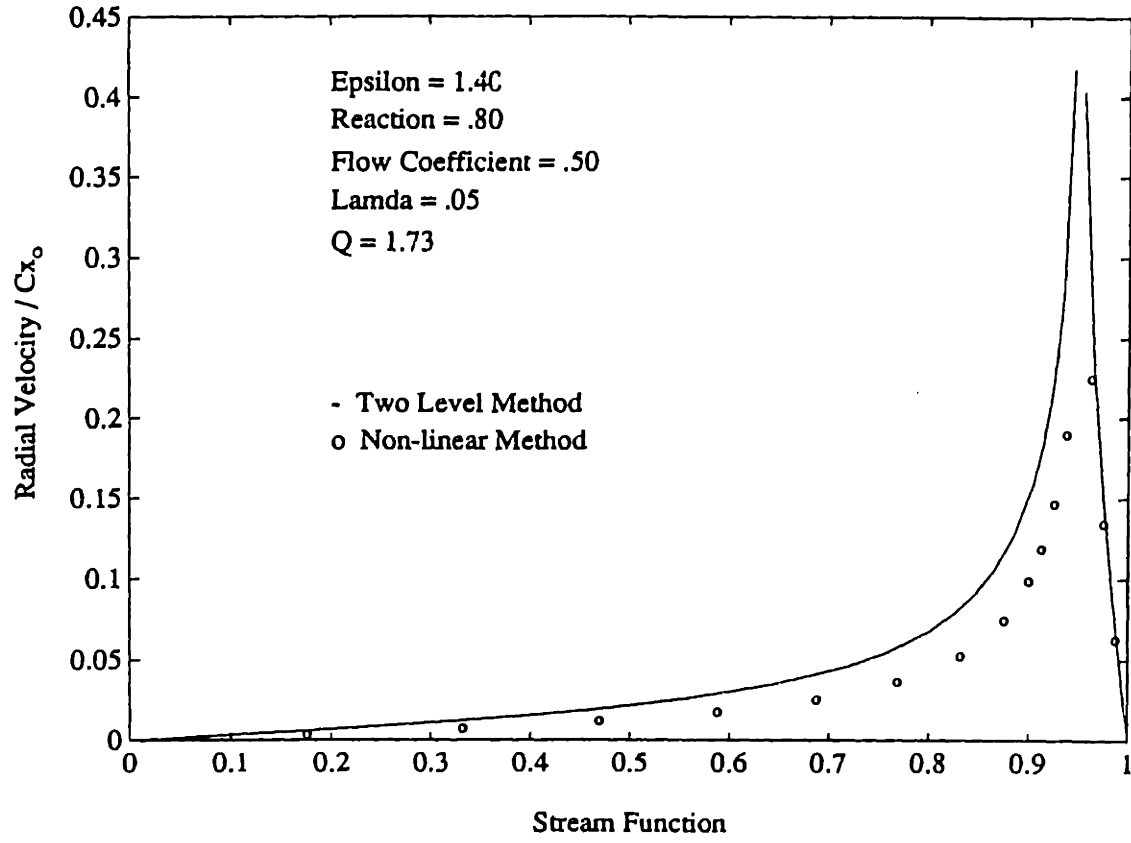


Fig. 3.13

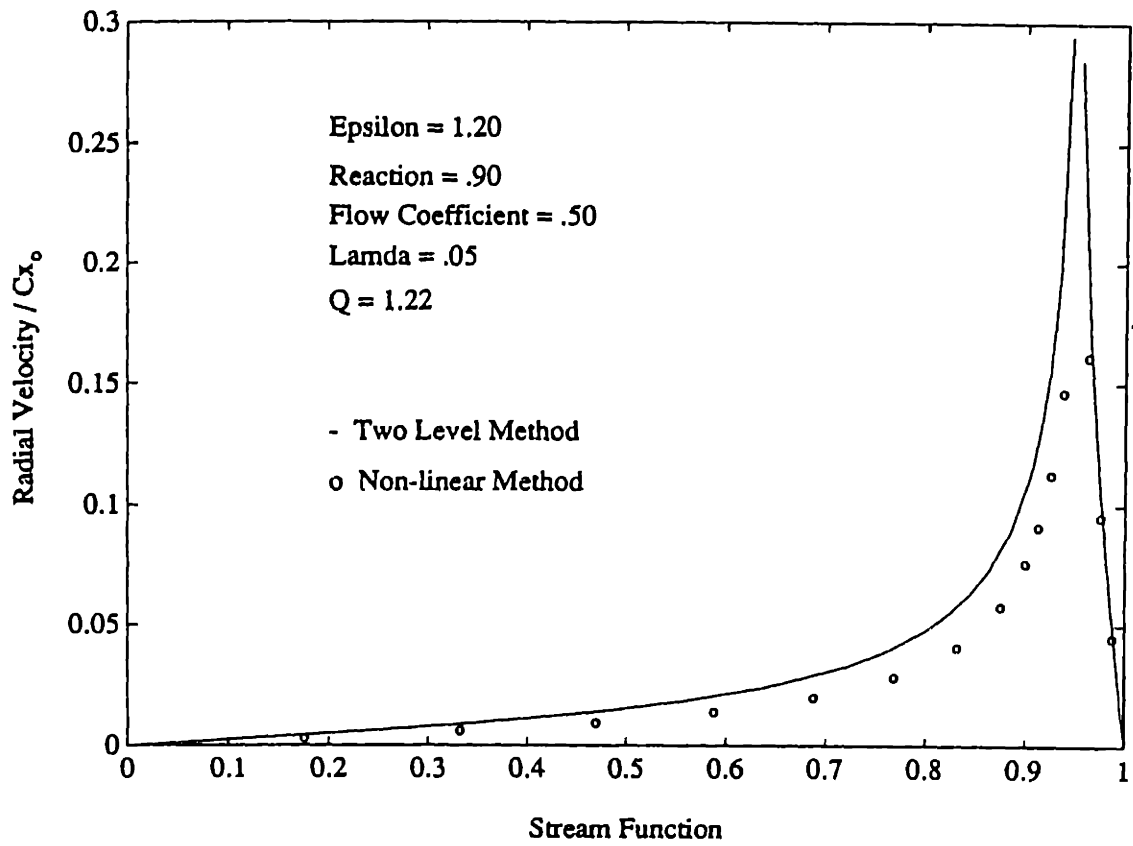


Fig. 3.14

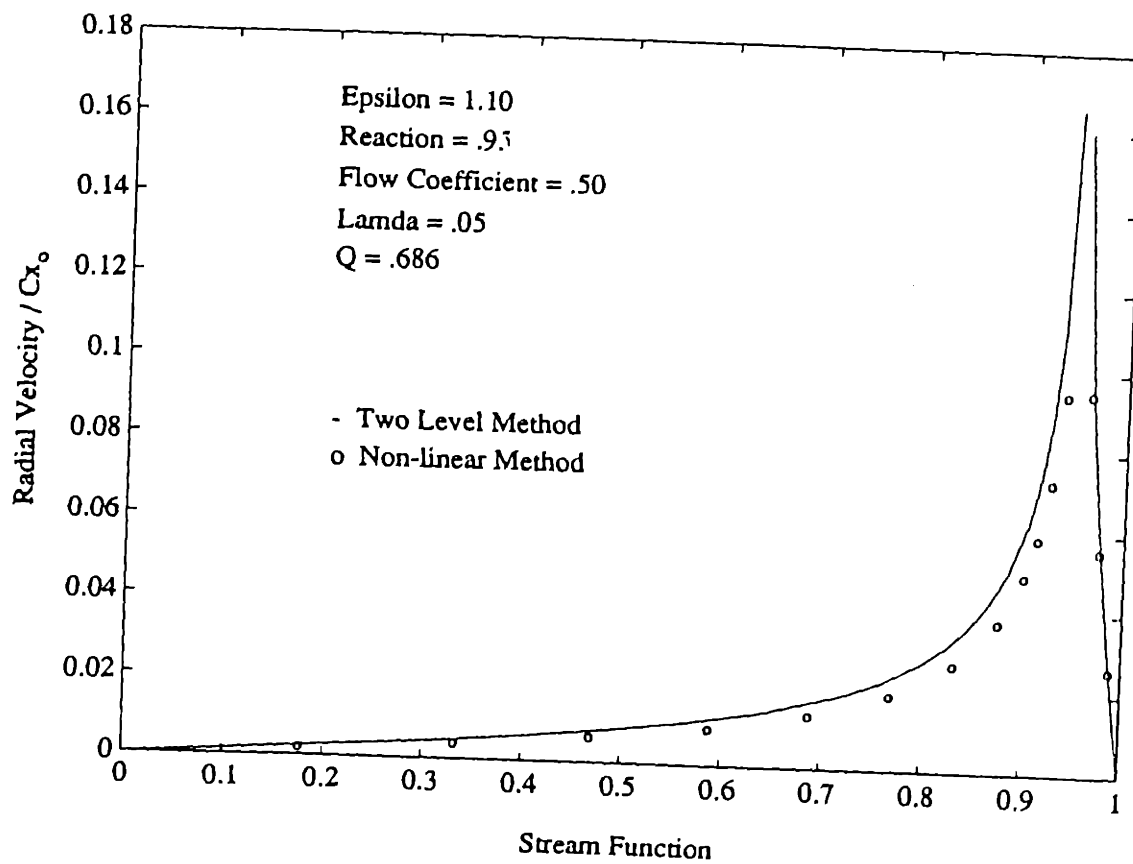


Fig. 3.15

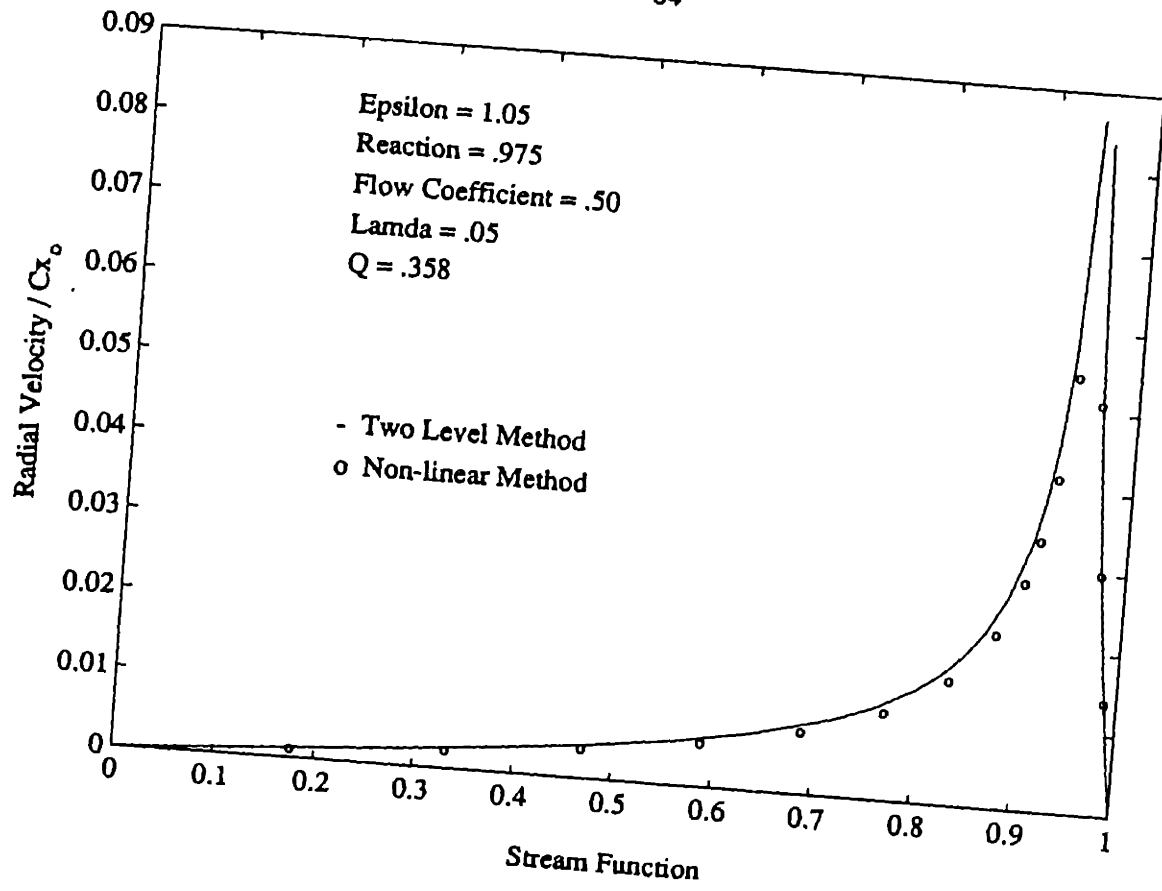


Fig. 3.16

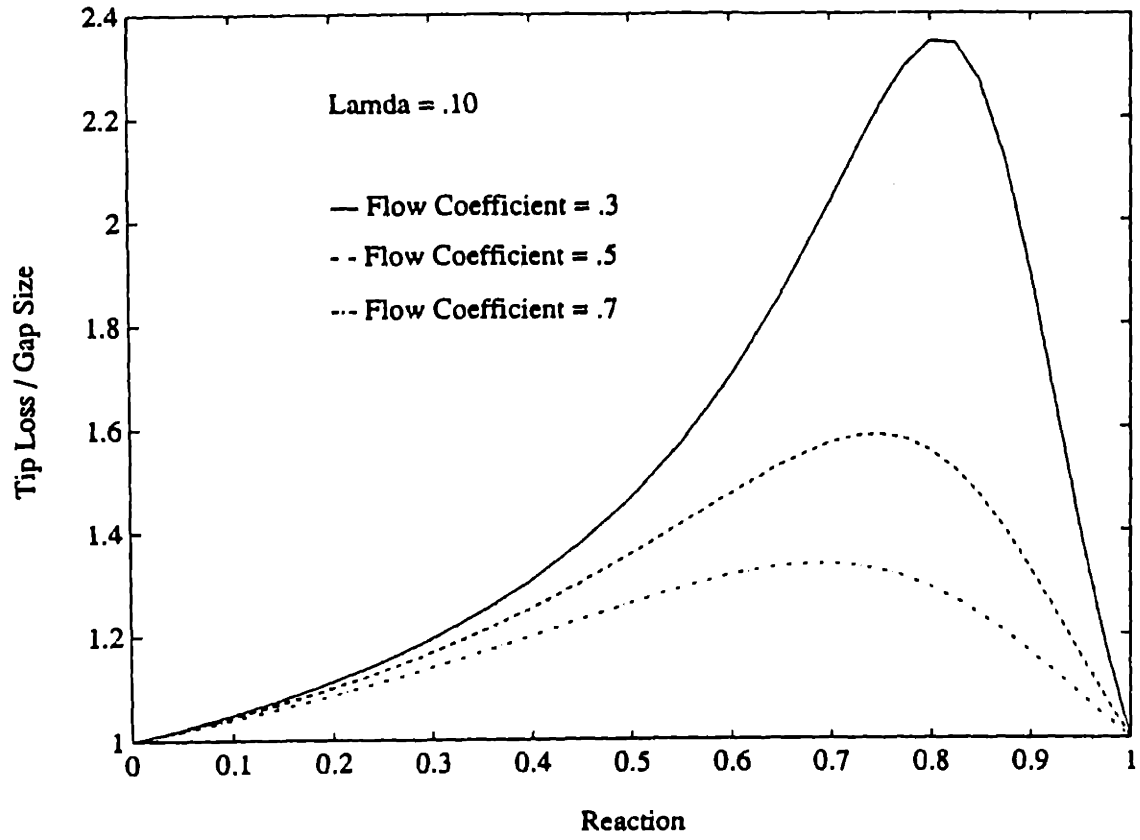


Fig. 3.17

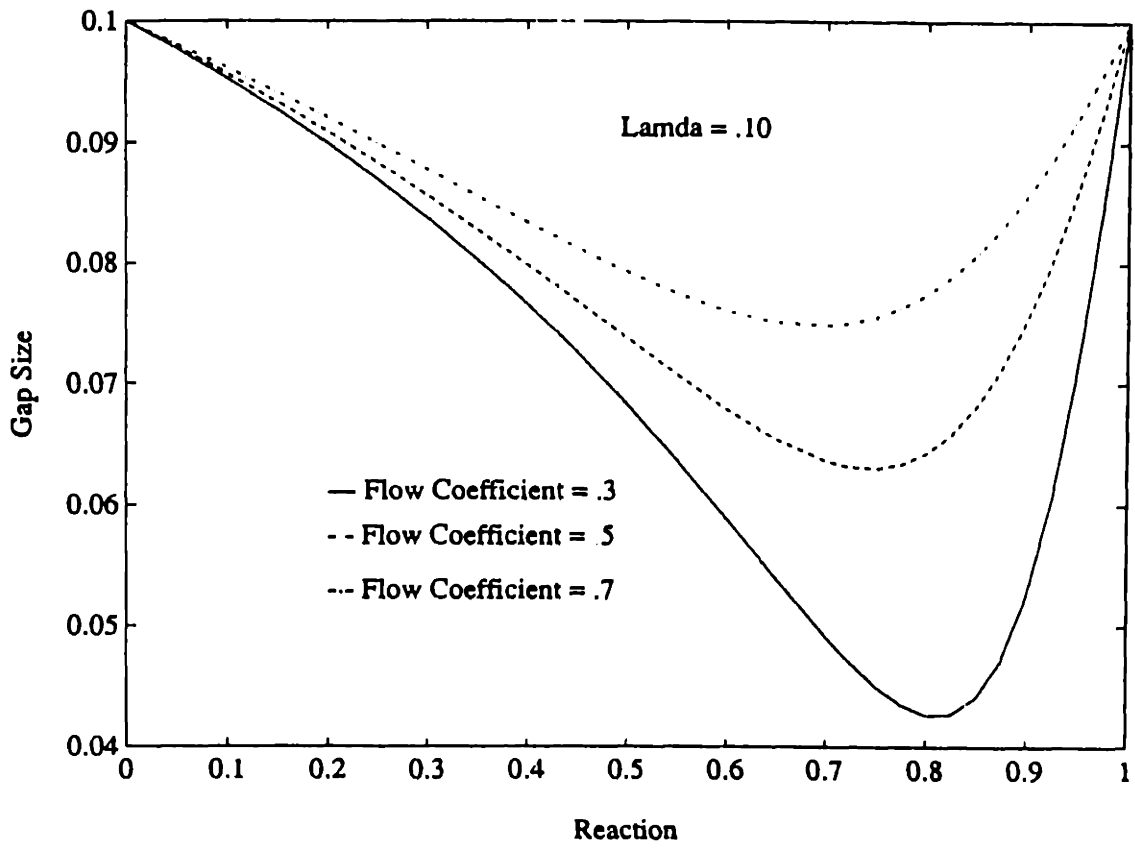


Fig. 3.18

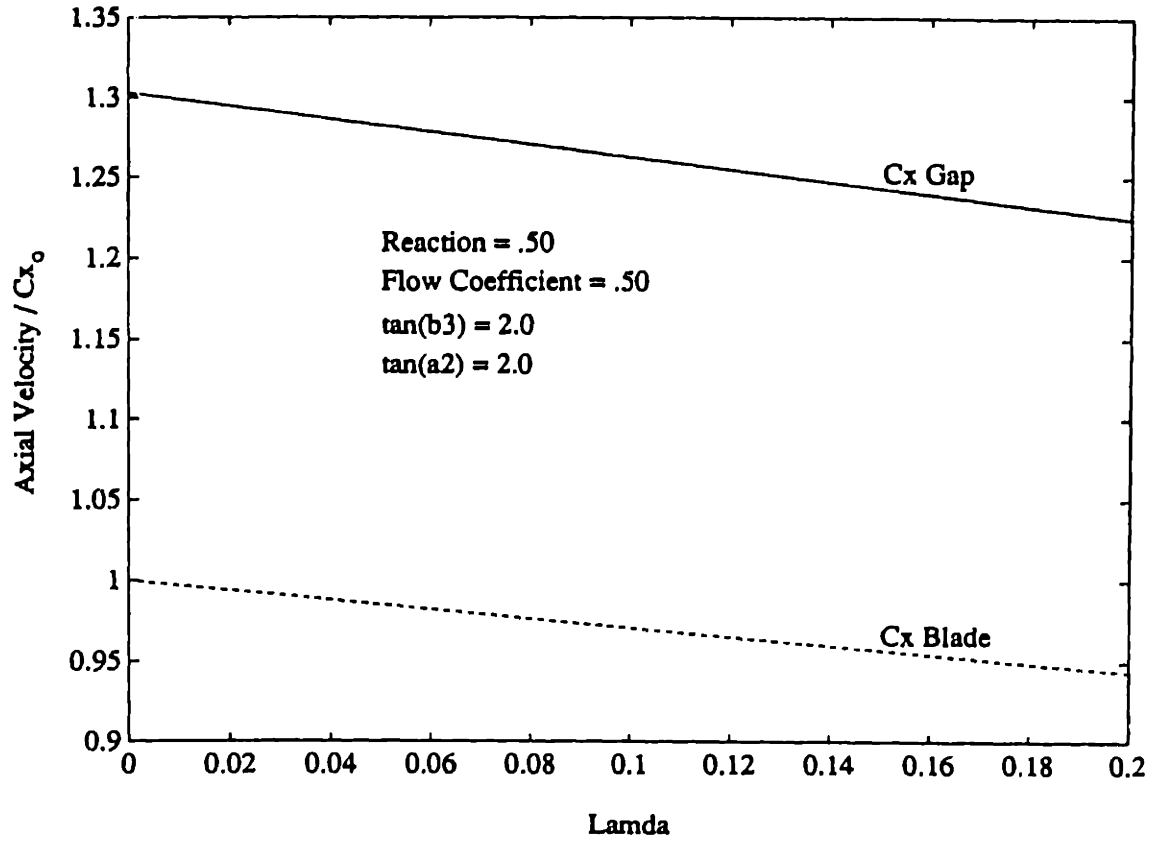


Fig. 3.19

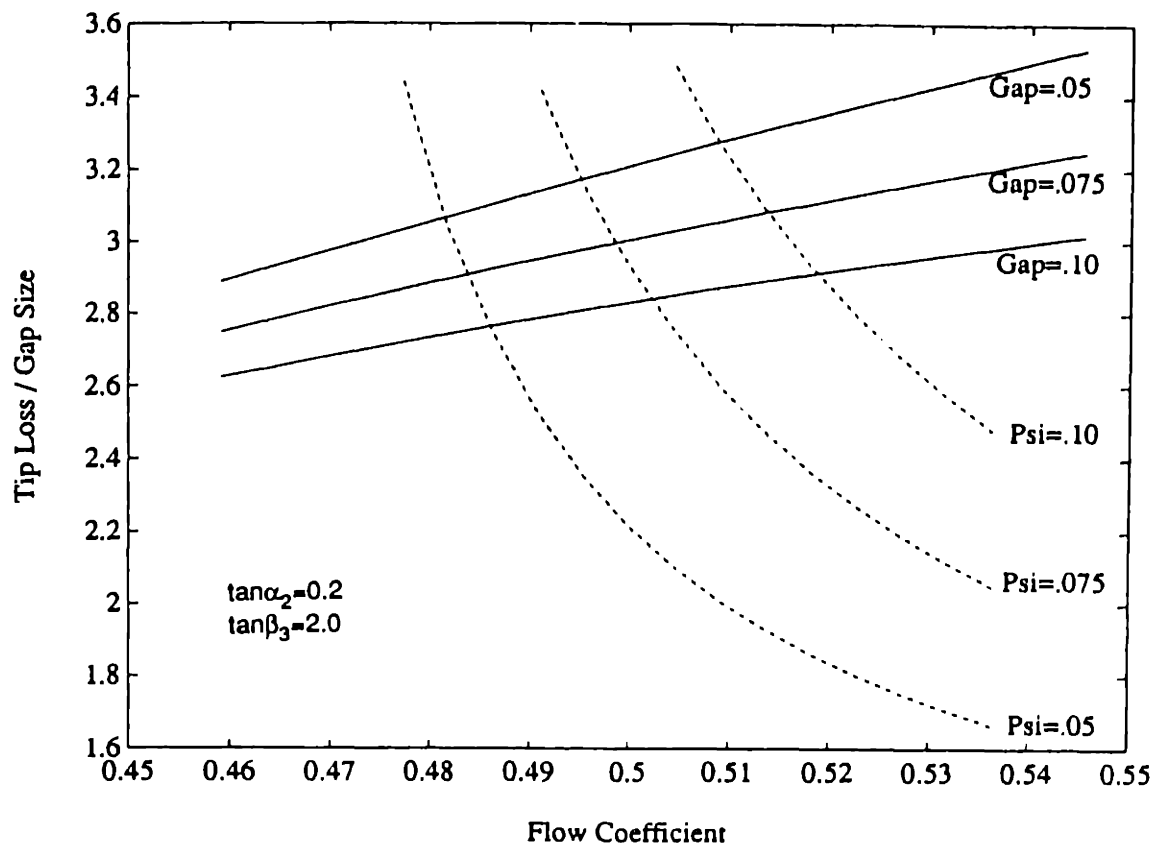


Fig. 3.20

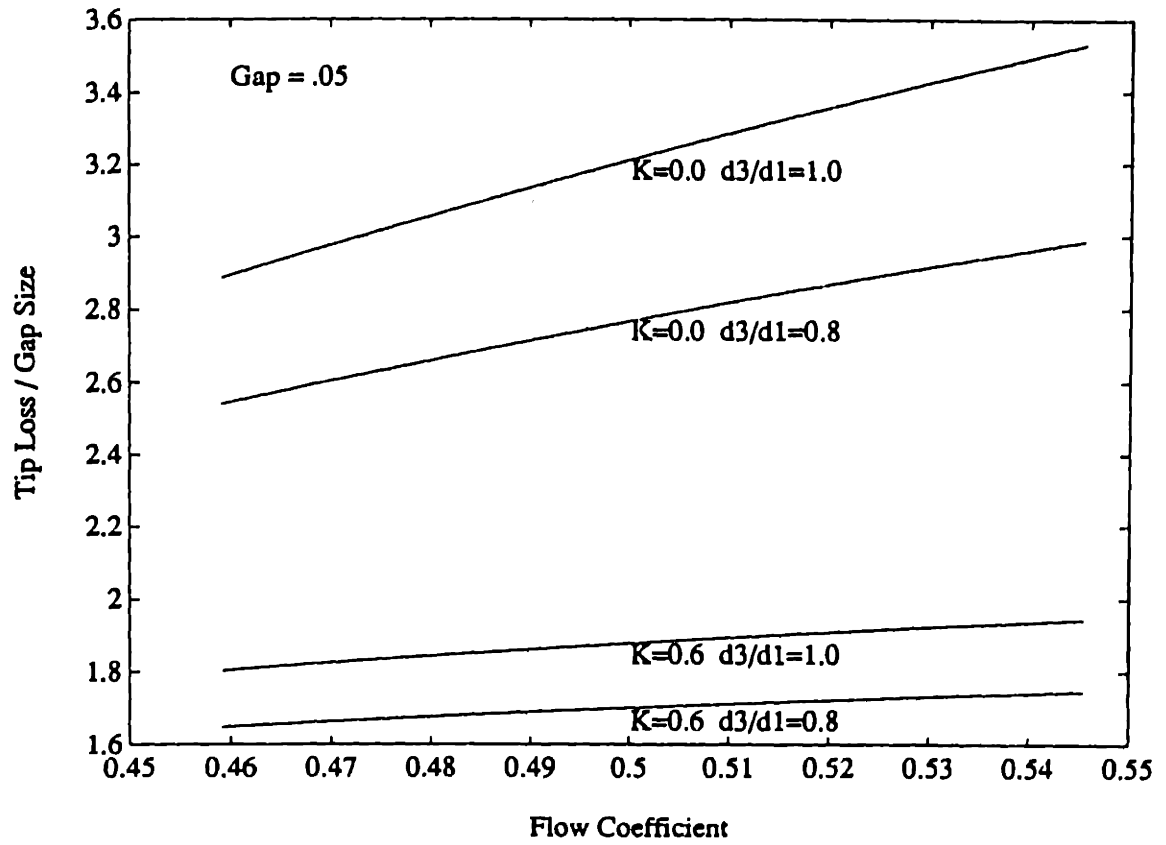


Fig. 3.21

Table 3.1 Axial and radial velocities at $x=0$ for two grid sizes

| | Grid 16X32 | Grid 24X48 |
|--------|---------------|---------------|
| ϕ | $(C_x)_{x=0}$ | $(C_x)_{x=0}$ |
| .9750 | 1.36396 | 1.36279 |
| .9250 | .97904 | .97962 |
| .9000 | .98285 | .98326 |
| ϕ | $(C_z)_{x=0}$ | $(C_z)_{x=0}$ |
| .9750 | .13404 | .13677 |
| .9250 | .14692 | .15054 |
| .9000 | .09922 | .09976 |


```

c   Update z on disc and calculate vorticity
cccccccccccccccccccccccccccccccccccccccccccccccccccccccccccc
      print*, 'ok'

512  do 540 j=1,n
      zd(j)=zd(j)/2+(z1(1,j)+zr(1,j))/4

      if(j .eq. n/4)go to 540

      kp=psi(j-1)-psi(j)
      if(j .eq. 1)then
        kp=1-psi(1)
      endif

      km=psi(j)-psi(j+1)
      if(j .eq. n)then
        km=psi(n)
      endif

      z0=zd(j)
      zdn=zd(j-1)
      if(j .eq. 1)then
        zdn=1
      endif

      zds=zd(j+1)
      if(j .eq. n)then
        zds=0
      endif

      zdpsi=(km/kp*zdn-kp/km*zds)/(kp+km)+(kp-km)*z0/kp/km
      zdpsi2=2*(zdn/kp+zds/km)/(kp+km)-2*z0/kp/km

      if(j .lt. n/4)go to 536

      vort(j)=(zdpsi*ta2/fi+tb3**2)*zapsi2/zdpsi**3
      cxd(j)=1/zdpsi
      go to 540

536  vort(j)=ta2**2*zdpsi2/zdpsi**3
      cxd(j)=1/zdpsi

540  continue

      do 80 j=1,n
c     print*, j,psi(j),zd(j),cxd(j),vort(j)
80   continue

cccccccccccccccccccccccccccccccccccccccccccccccccccccccccccc
c   Calculate shear strength
cccccccccccccccccccccccccccccccccccccccccccccccccccccccccccc

      jsh=n/4
      dpsi=psi(jsh)-psi(jsh+1)
      cx0g=dpsi/(zd(jsh-1)-zd(jsh))

```

```

cx0b=dpsi/(zd(jsh)-zd(jsh+1))
q=cx0b/fi*ta2-(1/fi**2-cx0b**2*tb3**2)/2-cx0g**2*ta2**2/2
q=(q+oldq)/2

c      print*, 'q =', q, cx0g, cx0b, zsh

      oldq=q
cccccccccccccccccccccccccccccccccccccccccccccccccccccccccccccccc
c      Update z along shear layer
cccccccccccccccccccccccccccccccccccccccccccccccccccccccccccccccc

      do 90 i=1,n
      zsh0=zr(i, jsh)
      zsh=zsh0

      hm=xr(i)-xr(i-1)
      if(i .eq. 1)then
        hm=xr(1)
      endif

      hp=xr(i+1)-xr(i)
      if(i .eq. n)then
        hp=hm
      endif

      zw=zr(i-1, jsh)
      if(i .eq. 1)then
        zw=zd(jsh)
      endif

      ze=zr(i+1, jsh)
      if(i .eq. n)then
        ze=zsh
      endif

      it=1

660   zx=(hm/hp*ze-hp/hm*zw)/(hm+hp)+(hp-hm)*zsh/hm/hp
      zsh=(zr(i, jsh+1)+zr(i, jsh-1))/2-q/dpsi**2/(zr(i, jsh+1)
&      -zr(i, jsh-1))*(zr(i, jsh+1)-zsh)**2*(zsh-zr(i, jsh-1))**2
&      /(1+zx**2)

      if(abs(1-zsh/zsh0) .lt. .001)go to 700

      hold=zsh-zsh0

      if(hold .gt. 0)then
        ppl=1
      else
        ppl=0
      endif

      if(hold0 .gt. 0)then
        pp2=1

```

```

else
  pp2=0
endif

if(pp1 .ne. pp2)then
  zsh=(zsh+zsh0)/2
elseif(zsh-zsh0 .gt. 0.0)then
  zsh=zsh-.0005
else
  zsh=zsh+.0005
endif

hold0=hold

zsh0=zsh

it=it+1
go to 660

700 zr(i, jsh)=zsh

90 continue

do 100 j=1,n
  do 110 i=1,4
c     print*, zr(i, j)
  110 continue
c     print*, zr(5, j)
  100 continue

cccccccccccccccccccccccccccccccccccccccccccccccccccccccccccccccc
c  Update z for interior points. First compute derivatives.
cccccccccccccccccccccccccccccccccccccccccccccccccccccccccccccccc

sum=0

do 120 i=1,n
  do 130 j=1,n

cccccccccccccccccccccccccccccccccccccccccccccccccccccccccccccccc
c  Derivatives downstream
cccccccccccccccccccccccccccccccccccccccccccccccccccccccccccccccc

  if(j .eq. jsh)go to 890

  hm=xr(i)-xr(i-1)
  if(i .eq. 1)then
    hm=xr(1)
  endif

  hp=xr(i+1)-xr(i)
  if(i .eq. n)then .
    hp=hm
  endif

  kp=psi(j-1)-psi(j)

```



```

if(j .eq. 1)then
  kp=1-psi(1)
endif

km=psi(j)-psi(j+1)
if(j .eq. n)then
  km=psi(n)
endif

z0=zr(i,j)
zn=zr(i,j-1)
if(j .eq. 1)then
  zn=1
endif

zs=zr(i,j+1)
if(j .eq. n)then
  zs=0
endif

zw=zr(i-1,j)
if(i .eq. 1)then
  zw=zd(j)
endif

ze=zr(i+1,j)
if(i .eq. n)then
  ze=z0
endif

zne=zr(i+1,j-1)
if(j .eq. 1)then
  zne=1
endif
if(i .eq. n)then
  zne=zn
endif

side=2

810  zx=(hm/hp*ze-hp/hm*zw)/(hp+hm)+(hp-hm)*z0/hp/hm
      zpsi=(km/kp*zn-kp/km*zs)/(km+kp)+(kp-km)*z0/kp/km
      zxx=2*(ze/hp+zw/hm)/(hp+hm)-2*z0/hp/hm
      zpsi2=2*(zn/kp+zs/km)/(kp+km)-2*z0/kp/km
      zxpsi=(zne-zn-ze+z0)/hp/kp
      lap=-zxx/zpsi+2*zx*zxpsi/zpsi**2-(1+zx**2)*zpsi2/zpsi**3

if(side .eq. 1)go to 980

if(i .eq. n)then
  cxinf(j)=1/zpsi
endif

resr=lap-vort(j)
ztr=-zpsi*resr

```



```

cccccccccccccccccccccccccccccccccccccccccccccccccccccccccccccccc
    if(j .gt. n/2)then
        dt=time + delte*(psi(j)-psi(j+1))
    else
        dt=time
    endif

    zl(i,j)=zl(i,j)+ztl*dt

    if(j .eq. jsh)go to 130

    zr(i,j)=zr(i,j)+ztr*dt

130    continue
120    continue

cccccccccccccccccccccccccccccccccccccccccccccccccccccccccccccccc
c   Calculate velocities at disc
cccccccccccccccccccccccccccccccccccccccccccccccccccccccccccccccc

    do 150 j=1,n

        zx=(zr(1,j)-zl(1,j))/(xr(1)-xl(1))
        czd(j)=zx*cxd(j)

        if(float(m)/50 .eq. int(float(m)/50))then
            print*, psi(j),zd(j),zx
        endif

150    continue

cccccccccccccccccccccccccccccccccccccccccccccccccccccccccccccccc
c   report velocities at disc and downstream
cccccccccccccccccccccccccccccccccccccccccccccccccccccccccccccccc

    if(float(m)/50 .eq. int(float(m)/50))then
        print*, ' '
        print*, m
    do 555 j=1,n
        print*, j,psi(j),cxd(j),czd(j),cxinf(j)
555    continue
        print*, ' '
        print*, 'sum of residues =',sum
    endif

    t=t+dt
    m=m+1

    go to 512

end

```